Time Series Assessment of Soil Erosion Risk Using RUSLE Model: A Machine Learning Approach: (a case study in Abaya Lake Sub-Catchment)

Tesfaye Abebe Tesema

A Thesis Submitted to the Department of Architecture

College of Civil Engineering and Architecture (CoCEA).

Presented in Partial Fulfillment of the Requirement for the Degree of Master's in Geoinformatics Engineering

Office of Graduate Studies

Adama Science and Technology University

May, 2025
Adama, Ethiopia

Time Series Assessment of Soil Erosion Risk Using RUSLE Model: A Machine Learning Approach (a case study of Abaya Lake Sub-Catchment"

Tesfaye Abebe Tesema

Advisors:

Temesgen Abraham Gebreselassie (Ph.D)

A Thesis Submitted to the Department of Architecture

College of Civil Engineering and Architecture (CoCEA).

Presented in Partial Fulfillment of the Requirement for the Degree of Master's in Geoinformatics Engineering (Specialization in GIS and Remote Sensing)

Office of Graduate Studies

Adama Science and Technology University

May,2025
Adama, Ethiopia

Declaration

Declaration I hereby declare that this Master Thesis entitled "-**Time Series Assessment of Soil Erosion Risk Using RUSLE Model: A Machine Learning Approach (a case study of Abaya Lake Sub-Catchment"**" is my original work. That is, it has not been submitted for the award of any academic degree, diploma or certificate in any other university. All sources of materials that are used for this thesis have been duly acknowledged through citation.

Tesfaye Abebe Tesema ____ ____________________ ______________________

Name of the student Signature Date

Recommendation

I/we, the advisor(s) of this thesis, hereby certify that I/we have read the revised version of the thesis entitled "**Time Series Assessment of Soil Erosion Risk Using RUSLE Model: A Machine Learning Approach (a case study of Abaya Lake Sub-Catchment** prepared under my/our guidance by **Tesfaye Abebe Tesema** submitted in partial fulfillment of the requirements for the degree of Mater's of Science in Geoinformatics Engineering, Specialization in GIS and Remote Sensing.

Therefore, I/we recommend the submission of revised version of the thesis to the department following the applicable procedures.

Major Advisor	Signature	Date
Co-advisor	Signature	Date

Approval

I/we, the advisors of the thesis entitled "_Time Series Assessment of Soil Erosion Risk Using RUSLE Model: A Machine Learning Approach: (a case study in Abaya Lake Sub-Catchment)" and developed by Tesfaye Abebe, hereby certify that the recommendation and suggestions made by the board of examiners are appropriately incorporated into the final version of the thesis.

Major Advisor	Signature	Date
Co-advisor	Signature	Date

We, the undersigned, members of the Board of Examiners of the thesis by Tesfaye Abebe have read and evaluated the thesis entitled "Time Series Assessment of Soil Erosion Risk Using RUSLE Model: A Machine Learning Approach: (a case study in Abaya Lake Sub Catchment)" and examined the candidate during open defense. This is, therefore, to certify that the thesis is accepted for partial fulfillment of the requirement of the degree of Master of Science in Geoinformatics Engineering.

Chairperson	Signature	Date
Internal Examiner	Signature	Date
External Examiner	Signature	Date

Final approval and acceptance of the thesis is contingent upon submission of its final copy to the Office of Postgraduate Studies (OPGS) through the Department Graduate Council (DGC) and College Graduate Committee (CGC).

Department Head	Signature	Date
College Dean	Signature	Date
Office of Postgraduate Studies, Dean	Signature	Date

ACKNOWLEDGMENT

I wish to express my deepest gratitude to my advisors **Dr. Temesgen Abraham** for his helpful nature and invaluable input in every stage of the study. I am really pleased to work this thesis under his guidance. I am also thankful to National Meteorological Service Agency (NMSA), for making available relevant data and documentation. Finally, my grateful thanks belong to my brother, Worku Abebe for his moral and support throughout the study.

Table of Contents **PAGE**

LIST OF TABLES

TABLE **PAGE**

LIST OF FIGURES

FIGURS **PAGE**

LIST OF ACRONYMS

FAO	Food and Agriculture Organization
IUCN	International Union for Conservation of Nature
RUSLE	Revised Universal Soil Loss Equation
SWC	Soil and Water Conservation
SDGs	Sustainable Development Goals
WEPP	Water Erosion Prediction Project
EUROSEM	European Soil Erosion Model
IAEA	International Atomic Energy Agency
PNAS	Proceedings of the National Academy of Sciences
NGOs	Non-Governmental Organizations
RF	Random Forest (a Machin Learning Algorithem)
GIS	Geographic Information System
IPBES	International Science-Policy platform on Biodiversity and Ecosystem Service
SSA	Sub-Saharan Africa
CIAT	International Center for Tropical Agriculture

ABSTRACT

The objective of this study was to examine the nature, extent and rate of soil erosion in Abaya Lake sub-catchment using model estimate and GIS. Revised Universal Soil Loss Equation (RUSLE) integrated with Machin learning approach; satellite remote sensing and geographical information systems (GIS) are used as a methodology. Annual precipitation, FAO digital soil map, 12.5m digital elevation model, land-cover map, land use types and slope steepness were used to determine the RUSLE factors. Findings indicated that, the total soil loss in the sub-Catchment amounted to 2.38 million tons per year, with potential annual soil loss varying from 0.0 to 508.97 tons/ha/year and average annual soil loss rate of 32.84 tons/ha/year, exhibiting notable spatial variability. Specifically, the average annual soil loss in the western catchment ranged from 0.0 to 507.97 tons/ha/year, while the upper and lower section of the Sub-catchment *showed average annual soil loss ranging from 0.0 - 101.1 and 0.0 - 64.94 tons/ha/year respectively. The study classified areas experiencing sever erosion covering approximately 13,724 hectares (16% of the total catchment), while regions at high and very high risk accounted for 62,707.5hecatrs (73%) and moderate risk covers 9,614.55hectars (11%). To facilitate effective soil and water conservation strategies, the sub-watersheds were prioritized based on erosion severity. The finding highlighted the critical need for conservation measures in areas classified as sever and very high risk to prevent irreversible degradation. Consequently, sub-watershed "A" was identified as the top priority for immediate conservation efforts followed by sub watershed "B", "G", and "D" in the second phase, with "H", "F" and "E" in the third phase and finally sub-watershed "C" last.*

Key words: Soil Erosion, RUSLE; GIS; Soil conservation; Machin learning

CHAPTER ONE

1. INTRODUCTION

1.1 Background and Justification

Soil erosion represents a pressing environmental challenge that significantly impacts global food security and ecosystem health. Defined as the process of soil removal from the land surface, erosion can occur naturally but is often exacerbated by unsustainable human activities such as intensive agriculture, deforestation, and overgrazing. These practices can increase erosion rates dramatically, sometimes by up to 1000 times the natural rate, leading to severe degradation of soil resources (Tatjana D. et al, 2022).

Reports from the Food and Agriculture Organization (FAO) emphasize that current erosion rates far exceeded the rate of soil formation, rendering soil a finite resource with degradation often irreversible within a human lifetime (FAO, 2015; FAO, 2020).

The consequences of this phenomenon are extensive, resulting in diminished agricultural productivity, impaired ecosystem functions, increased risks of landslides and floods, significant biodiversity loss, and even community displacement.

According to IUCN (2015), Water erosion globally accounts for the majority of soil degradation, affecting Asia and Africa most severely. Based on IUCN predication, if the current trend of soil erosion continued, over 90% of the earths land could experience a very significant land degradation by 2050, with potential displacing millions of people and reducing global agricultural yield by an average of 10% (Nachtergaele et al., 2012; IUCN, 2015). In Ethiopia, where agriculture is solely dependent of rain feed, soil erosion poses a critical threat to food security and sustainable land management (Dofee and Goshu, 2024).

According to Humbo Woreda 2020 Disaster risk profile report, Soil erosion was identified as the major environmental issues caused by factors like, population pressure, unsustainable agricultural practices and deforestation. Other similar research's also shown soil degradation which is manifested by topsoil loss and gully formation is severely impacting the livelihood of the local community. Despite existing studies demonstrating the effectiveness of certain soil and water conservation measures in improving soil properties, there remains a significant gap in quantitative assessments of annual soil loss in Humbo Woreda.

Recent research findings that used the traditional Universal Soil Loss Equation has highlighted, high erosion risks owing to different environmental factors. However, as a result of advancement in technology, now there is a need for comparative studies which incorporates Machin learning models such as "Random Forest" and enhance the accuracy of soil erosion quantitative measures.

The use of machine learning algorithms such as Random Forest (RF) has become popular due to their ability to delineate complex landscapes at a high level of detail, and with better accuracies (Goldblatt et al.,2016).

Therefore, this research aims to assess the magnitude, rate and dynamics of soil erosion in Abaya Lake sub-Catchment by using the traditional RUSLE model integrated with RF Machin learning algorism and GIS analysis. Ultimately, this effort will yield valuable insights for local Natural resource managers and policymakers, and NGOs, aiding them in their initiatives to combat soil erosion and foster sustainable land use practices.

1.2 Statement of the Problem

Soil Erosion is one of the pressing environmental problems, that significantly endangers global food security and the health of ecosystem. While it is a natural process, it is intensified by unsustainable human practices such as intensive agriculture, deforestation, overgrazing, and improper land use changes. These activities can uplift erosion rate by as much as 1000 times beyond natural levels, resulting in sever degradation of soil resources. According to the world soil status report, soil erosion is identified as a major threat to soil health (FAO,2015a), with current erosion rates vastly outpacing the rate of soil formation. This unsustainable depletion makes soil a finite resource, and its degradation is often irreversible within a human lifetime (FAO, 2020).

The consequences of soil erosion are profound and multifaceted. They include reduced agricultural productivity, impaired ecosystem functions, increased hydrogeological risks such as landslides and floods, significant biodiversity loss, damage to urban infrastructure, and in extreme cases, the displacement of communities (FAO, 2020). Furthermore, soil erosion directly threatens global food security and undermines efforts to achieve the Sustainable Development Goals (SDGs), which aim to enhance the well-being of over 3.2 billion people worldwide (UN, 2015; FAO, 2020).

Globally, water erosion accounts for the majority (56%) of soil degradation, followed by wind erosion (28%) and nutrient decline (7%). The most affected regions include Asia and Africa for water erosion and Asia for wind erosion. Alarmingly, projections indicate that future land degradation will primarily impact areas with substantial arable land remaining. If current trends persist, it is estimated that by 2050, over 90% of the Earth’s land areas will experience significant degradation. This scenario could force 50–700 million people to migrate due to environmental pressures and reduce global crop yields by an average of 10%, with some regions facing declines of up to 50% (Nachtergaele et al., 2012; IUCN, 2015; Gomiero, 2016; IPBES, 2018). Annually, approximately 75 billion tons of fertile soil are lost due to erosion, equating to a loss of about 12 million hectares of land each year (FAO and IAEA, 2017).

In developing countries like Ethiopia, the impact of soil erosion is particularly severe due to a direct dependence on soil for livelihoods. Erosion reduces the effective rooting depth of soils, depletes organic matter and nutrients, and diminishes water retention capacity. The primary drivers of this degradation in Ethiopia include population pressure, agricultural mismanagement, deforestation, and overgrazing (Habtamu et al. (2020). The average annual rate of soil loss in Ethiopia is estimated at 12 tons per hectare (Feyera, 2021).

As it is documented on Humbo Woreda Disaster Risk Profile (2020), soil erosion is one of the several escalating environmental problems in the region. Factors such as deforestation and overgrazing contribute significantly to this issue by depleting soil fertility and increasing food insecurity among local communities.

In line with the above, historical record indicate that in 2003, a voluntary resettlement initiative took place for farmers from overpopulated areas. As a result, Humbo woreda become home to 658 households (Un, 2003). These families were selected from densely populated areas of Humbo, Boloso Sore, Kindo Koysha, Sodo Zuriya, Damote Weyde, and Damote Gale, and they were resettled in a new village located in the southeastern part of the woreda, near lake Abaya, starting in May 2003 (UN, 2003). The researcher believes that, this resettlement has contributed to soil degradation in the Abaya Lake sub-Catchment.

A Research conducted by Meseret et al (2019), in Humbo Woreda indicates that land degradation manifests not only through topsoil loss but also through gully formation and declining soil health. Despite his study showing that specific Soil and Water Conservation (SWC) measures, such as soil bunds and trenching, can improve certain soil properties by enhancing organic carbon levels and reducing bulk density in conserved lands compared to non-conserved plots (Meseret et al., 2019), there remains a critical lack of quantitative assessments regarding annual soil loss in Humbo Woreda.

Another study conducted in Abaya Lake catchment by Shibire, et al (2024), used the Revised Universal Soil Loss Equation (RUSLE), to assess annual soil loss and erosion risk. According to his finding, a significant portion of the catchment was categorized under high risk of erosion due to factors such as land use, slope, and vegetation cover. But a potential research gap lies in the comparison of RUSLE model integrated with machine learning approach such as the Random Forest classifier for quantifying soil erosion.

Integrating the Revised Universal Soil Loss Equation (RUSLE) model with machine learning, specifically the Random Forest (RF) algorithm, is essential for enhancing the accuracy and reliability of soil erosion quantification. Traditional RUSLE relies on empirical relationships and linear assumptions that may not fully capture the complex, non-linear interactions among various environmental factors influencing soil erosion. Recent studies have demonstrated that machine learning models, such as RF, can significantly outperform traditional methods in predicting soil loss by effectively handling large datasets and identifying intricate patterns within them. For instance, research indicates that RF models have achieved high accuracy rates, with some studies reporting an Area Under Curve (AUC) value of 98% in predicting susceptibility to water erosion, showcasing their robustness compared to conventional approaches (Al-Abadi & Al-Ali, 2018; Azedou et al., 2021).

Additionally, Machin learning techniques can integrate a wider array of variables, such as topography, land use and climate data, which are often challenging to measure with conventional models. This ability enables a more thorough analysis of the factors contributing to soil erosion in particular areas. For instance, a recent study demonstrated that, combining Random Forest (RF) with the Revised Universal Soil Loss Equation (RUSLE) not only enhanced predictive accuracy but also shed light on the key drivers of soil erosion by examining several influencing factors at once (Wang et al., 2016; Mohebzadeh et al., 2022).

In this study, the researcher combined Machin learning techniques with the Revised Universal Soil Loss Equation (RUSLE) to accurately estimate annual soil loss in the study area from 2003 to 2025, considering the 2003 resettlement as a baseline. This integration is especially important in regions such as Abaya Lake sub-Catchment, where precise assessment of soil erosion is essential for improving agricultural sustainability and food security amid ongoing environmental challenges.

1.3 Objectives of the study

1.3.1 General Objective of the Study

The general objective of this study is to assess the extent and rate of water erosion (rill and sheet erosion) risk and the dynamic change of spatial distribution and temporal variation in erosion status and intensity over time in Abaya Lake sub-Catchment, using RUSLE model integrated with Machin learning and GIS techniques.

1.3.2 Specific Objective

- To examine the extent and rate of soil erosion
- To assess soil erosion trend and its dynamics overtime (over the past 30 years)
- To Identify the critical watershed for intervention

1.4 Research Question

1. What is the magnitude and rate of soil loss in Abaya Lake sub basin?
2. What are the dynamics in soil erosion rate/loss in the sub basin?
3. Which part of the catchments are more exposed for a high soil erosion loss?

1.5 Significance of the research

The dynamic nature of erosion and associated processes and their dependence on climatic, pedo-logical, land cover, land use, and management factors result in spatial and temporal variability. Computing and mapping this variability will produce information which is essential for designing soil conservation management plans, and the evaluation of on-site and off-site damages by soi1 erosion, land use projects, and transport of pollutants. Furthermore, the information on the extent, severity and geographic distribution of degraded lands is of paramount importance for planning reclamation strategies and setting up preventive measures for sustainable agriculture development.

They become a significant basis for planners in drafting and implementing development plans for sustainable use of land resources as well for resource restoration and quality enhancement.

Therefore, the findings from this study will primarily benefit the Woreda land managers and NGOs which have implemented land resource management programs in the woreda, as it evaluates the impact of their program on the well-being of land and will suggest some key issues for further redesign. Furthermore, policy-makers, development planners, local land-mangers, concerned NGOs and any responsible bodies which can start water and soil conservation programs will be simply equipped to take appropriate decisions.

It will also have significance for future researcher to expand soil erosion assessment that integrate the traditional RUSLE model with Machin learning tools and enhance accuracies in estimating soil erosion

1.6 Delimitation Scope

This study is, actually a local level study and thus has focused mainly on issues related with the extent and dynamics of soil erosion in Abaya Lake sub-catchments. The study mainly focused on quantifying the amount of soil loss caused by sheet erosion.

1.7 Limitation of the Study

This study only focuses on sheet erosion using the Revised Universal Soil Loss Equation (RUSLE). While RUSLE serves as a valuable tool for estimating soil erosion potential based on the environmental variables, it does not account for a wider range of influences that contribute to erosion process. Notably, socio-economic factors such as land use practices, agricultural management techniques, and community involvement are not considered, even though they can play a critical role in soil conservation and erosion rates. As a result, the finding may not fully reflect the complexity of erosion dynamics within the study area.

1.8 Expected outcome of the study

The anticipated outcomes of this study on soil erosion risk assessment using the RUSLE model and machine learning techniques are multifaceted and aim to contribute significantly to both academic knowledge and practical applications in land management. Therefore, the expected outcome of the study include: -

- Quantified amount of soil loss and rate in the sub basin
- Identifies the hotspots and prioritized the sub watershed for future soil and water conservation management measures.
- The finding is a key resource for natural resource managers, policy makers and NGOs for planning.

1.9 Operational Definitions

To ensure clarity and precision throughout this research document, the following operational definitions are provided:

- **Soil Erosion**: The process by which soil is removed from the land surface by natural forces such as water or wind, often exacerbated by human activities like deforestation and intensive agriculture.
- **RUSLE (Revised Universal Soil Loss Equation)**: A widely used empirical model for estimating soil erosion rates based on factors such as rainfall intensity, soil type, topography, land use, and vegetation cover.

- **Machine Learning**: A subset of artificial intelligence that involves algorithms capable of learning from data to make predictions or decisions without being explicitly programmed for specific tasks.
- **Random Forest Classifier**: A machine learning algorithm that utilizes multiple decision trees to improve prediction accuracy by aggregating their outputs, particularly effective in handling complex datasets with numerous variables.
- **Watershed**: An area of land where all precipitation collects and drains into a common outlet, such as a river or lake. In this study, it refers specifically to regions within Humbo Woreda that are analyzed for soil erosion risk.
- **Soil Water Conservation (SWC)**: Practices aimed at managing water resources effectively to prevent soil degradation and enhance agricultural productivity. Examples include terracing, contour farming, and vegetative barriers

1.10 Organization of the Thesis

The thesis is organized into five chapters. Chapter 1 deals with the background and Justification, statement of the problem, objectives, scope and limitation, significance of the study and organization of the thesis. Chapter two reviews related literature. Methodological issues including the study area description were presented in chapter three. The fourth chapter presents the results and discussions of the study. The fifth chapter includes conclusion and recommendations.

CHAPTER TWO

2. LITERATURE REVIEW

2.1 Introduction to Soil Erosion

According to a Pereira and Muñoz-Rojas (2017) synthesis, “soil erosion is one of the major causes, evidence of, and key variables used to assess and understand land degradation”. It represents the process of top soil removal from the land surface through natural forces such as water and wind, which is often aggravated by human activities, that include forest clearing, overgrazing, and unsustainable agricultural practices (Borrelli et al., 2021; Mengie et al., 2021).

According to the World Bank report, approximately 1.5 billion people worldwide are affected by soil erosion, resulting reduction in agricultural production and posing magnificent threats to food security (World Bank, 2021).

Soil erosion in sub-Saharan Africa (SSA) and Ethiopia has reached its critical level, driven by a combination of climatic, topographic and anthropogenic factors. In Sub-Saharan, 65% of croplands experience erosion and runoff, with soil degradation are exceeding natural regeneration by 100-fold, costing the region $68Billion annually in lost agricultural productivity (CIAT, 2024).

In Ethiopia, where agriculture is predominantly rain-fed, soil erosion represents a severe risk to food security and sustainable land management practices (Abebe et al., 2020). Understanding the dynamics of soil erosion through time series analysis is crucial for developing effective management strategies that address these challenges.

2.2. Global Trends in Soil Erosion

According to the FAO (2020), Soil erosion is defined as the accelerated removal of topsoil through water, wind and tillage, poses a significant threat to global food security and sustainable development (FAO, 2020). Approximately (95% of the food consumed worldwide is derived from soil. Highlighting the critical need for effective soil erosion mitigation strategies, particularly through sustainable soil management (SSM) practices (FAO, 2020)

As documented by FAO (2020), Soil erosion occurs naturally under all climatic conditions and on all continents, but is significantly increasing and accelerated by unsustainable human activities, up to 1000 times from its natural level. These is due to intensive agriculture, clearing of forest, overgrazing and improper land use changes. The Status of the World’s Soil Resources report also identified soil erosion as one of the major soil threats (FAO, 2015a). Soil erosion rates are much higher than soil formation rates; soil is a finite resource, meaning its loss and degradation is not reversable within a human lifetime (FAO, 2020).

If the current soil erosion trend continued, from the total earth's soils, 33% are already degraded and predicted over 90% could become degraded by 2050, leading 4 billion people to live in drylands, 50–700 million people will be forced to migrate, and global crop yields will be reduced by an average of 10% and up to 50% in some regions (Nachtergaele et al., 2012 cited by Little, 2019; IUCN, 2015; Gomiero, 2016; IPBES, 2018).

2.3 Causes and Magnitude of Soil Erosion in Ethiopia

Several documents indicate, soil erosion in Ethiopia is primarily driven by both natural and anthropogenic factors (FAO, 2017; Hurni, 1988). Water-induced soil erosion is the most significant contributor to land degradation in the country, aggravated by rapid population growth, deforestation, overgrazing, and inadequate vegetative cover (Mengie et al., 2021; FAO & IAEA, 2017).

According in to Dereje eat al., (2006), the government of Ethiopian first recognized the severity of soil degradation following the devastating famine of 1973-1974. Since then, various soil and water conservation measures have been implemented; however, their adoption has not always met expectations due to socio-economic challenges (Dereje et al., 2006). Several recent assessment results indicated that, Average annual soil loss rates have increased significantly over the past few decades, with some regions experiencing losses exceeding 56 tons per hectare per year (Mengie et al., 2021).

2.3.1 Types of Soil Erosion: Causes and Consequences

Understanding the different types of erosion is crucial. For this specific study, the following soil erosion types are discussed below as it is referred from SOLitude Lake Management (2025).

a. **Type and Causes**
   - **Splash Erosion:** is one type of soil erosion caused by raindrops falling onto the land, causing topsoil to disintegrate into tiny, individual particles. The detached particles then form a crust on top that easily flows off when it is rainy or windy (SOLitude, 2025).
   - **Sheet Erosion**: - occurs when the thin upper portion of the soil is displaced, usually due to heavy rain or water runoff. This kind of soil erosion is gradual and often goes unnoticed until large portions of soil are displaced (SOLitude, 2025).

- **Rill Erosion:** - Shallow drainage channels that forms as rainwater flows into depression in the land. Over time, the depression created by this type of soil erosion can widen during each rainstorm, which in turn, can make the landscape even more prone to erosion (SOLitude, 2025).
- **Gully Erosion:** - occurs when runoff flows strongly and is concentrated in one location. In many cases, gullies begin as a rill that transitions into a small "waterfall" that is strong enough to eat away topsoil. As water picks up energy, the gully's slopes become steeper. This type of soil erosion is very visible and damaging. It often has a drastic effect on the productivity of the soil and can make the land unusable (SOLitude, 2025).

b. Soil Erosion consequences

Soil erosion in Ethiopia is not only an environmental concern, but also, an economic and social crisis that threatens agricultural production and local economies on a large scale. According to Wassie, (2020) as cited by Degfie and Tarekegn (2025), "the Ethiopian highlands are facing a staggering reduction in agricultural productivity which accounts 20% due to soil erosion, which is approximately costing $1.2 billion in agricultural output alone". According to Reda and Hailu, (2017), the cumulative direct costs, which includes the diminution of topsoil nutrients and lowered livestock capacity, have reached $7 billion in a single decade (2000–2010), with indirect costs from reduced water quality and infrastructure damage compounding this burden (Reda et al., 2017).

The consequences of erosion extend far beyond agriculture. As documented by Kidane and Alemu, (2015), Sedimentation in reservoirs, for instance, has reduced storage capacity by up to 30%, undermining Ethiopia's water management infrastructure and hindering development (Kidane et al., 2015).

2.4. Models for Assessing Soil Erosion

Numerous models have been developed to assess soil erosion risk effectively. The Revised Universal Soil Loss Equation (RUSLE) remains one of the most widely used empirical models for estimating soil loss based on various factors such as rainfall erosivity, soil erodibility, slope length and steepness, cover management, and conservation practices (Wischmeier & Smith, 1978, Renard et al., 1997). However, it has notable limitations that can affect its accuracy and applicability. One major drawback is its reliance on average annual estimates, which can obscure the spatial and temporal variability of erosion influenced by factors such as climate, land use, and management practices. For instance, RUSLE often underestimates erosion severity in dynamic environments, as it does not adequately account for the complex interactions among various factors that contribute to soil loss over time (Benavidez et al., 2018; Naipal et al., 2014).

Other models include the Water Erosion Prediction Project (WEPP) model and the European Soil Erosion Model (EUROSEM), each offering unique advantages depending on the specific context of study (Morgan et al., 1998; Nearing et al., 1999). These models are crucial for informing land management decisions and developing effective conservation strategies.

2.5. Digital Image Processing in Land Use/Land Cover Classification

Digital image processing plays a vital role in land use/land cover classification by enabling researchers to analyze satellite imagery effectively. Techniques such as supervised classification allow for distinguishing between different land cover types based on spectral signatures derived from remote sensing data (Lillesand et al.015). For instance, Landsat imagery has been widely used for classifying land cover types relevant to soil erosion assessments (Haregeweyn et al., 2017; Moges et al., 2021). Accurate classification is essential for understanding how different land uses influence soil erosion dynamics. Furthermore, accuracy assessment methods such as Kappa statistics provide a quantitative measure of classification accuracy, allowing researchers to evaluate how well their models perform against ground truth data (Congalton & Green, 2009).

2.5.1 Accuracy Assessment Related to Machine Learning-Based Classification

Machine learning techniques have emerged as powerful tools for improving classification accuracy in land use/land cover studies. Random Forest (RF), in particular, has gained popularity due to its robustness against overfitting and its ability to handle high-dimensional datasets effectively. Studies have shown that RF classifiers achieve high accuracy rates when applied to remote sensing data for land cover classification (Liaw & Wiener, 2002; Zhang et al., 2018). Accuracy assessment metrics such as overall accuracy and Kappa coefficient are commonly used to evaluate model performance. For example, a recent study demonstrated that an RF classifier achieved an overall accuracy of over 90% when classifying land cover types in Ethiopia using high-resolution satellite imagery (Yonas et al., 2021).

2.6 Remote Sensing and GIS Applications in Soil Erosion Assessment

Remote sensing technology combined with GIS has revolutionized soil erosion assessment methodologies. These tools enable researchers to collect large-scale spatial data efficiently to derive RUSLE parameters. For instance, satellite imagery can provide insights into changes in vegetation cover over time, which directly influence the C factor in RUSLE calculations (Milward & Mersey, 1999; Bahadur et al., 2012). Digital Elevation Models (DEMs) facilitate calculations of slope length and steepness factors necessary for RUSLE applications (Prasannakumar et al., 2012). The integration of remote sensing with GIS not only enhances the accuracy of erosion assessments but also allows for continuous monitoring of soil loss dynamics across different landscapes (Ji, et al.,2024).

2.7 Incorporating Machine Learning into Soil Erosion Modeling

The integration of machine learning techniques with traditional models like RUSLE represents a promising approach to enhance soil erosion predictions. Machine learning algorithms can analyze complex datasets to identify patterns and relationships that may not be evident through conventional statistical methods. Recent research has shown that machine learning models outperform traditional methods in predicting soil erosion when trained on high-resolution spatial data (Ganasri & Ramesh, 2016; Mohamad et al., 2021). For example, hybrid approaches combining machine learning with RUSLE have demonstrated improved accuracy in predicting soil loss rates compared to using RUSLE alone (Golkarian et al., 2023).

2.7.1 Suitable Machine Learning Tools for Soil Erosion Assessment

In ArcGIS Desktop, several machine learning tools can be employed for assessing soil erosion risk. Random Forest (RF) stands out as one of the most suitable classifiers due to its robustness against overfitting and its ability to handle large datasets with complex relationships between variables. Studies have indicated that RF consistently yields high accuracy rates when applied to remote sensing data for LULC classification and subsequent soil erosion modeling (Liaw & Wiener, 2002; Zhang et al., 2018). Additionally, Support Vector Machines (SVM) have also been effective in classifying land cover types relevant to soil erosion assessments (Mountrakis et al., 2011). However, RF's interpretability and ease of use make it particularly advantageous for researchers working within ArcGIS environments (Belgiu & Drăguţ, 2016).

CHAPTER THREE

3. MATERIALS AND METHODS

3.1 Description of the Study Area

Humbo is one of the woredas in the South Ethiopia Regional State. It is a Part of the Wolayita Zone located in the Great Rift Valley, bordered on the southeast by Abala Abaya, on the south by the Gamo Zone, on the west by Offa, on the north by Sodo Zuria and Bayra Koysha. Geographically, it is located at 6^0 43'44 N latitude and 37^0 45'51'' E longitude with an altitudinal range between 1100-2335m a.s.l.(Fekadu, 2014). Figure below shows map of the Study Area.

Figure 3.1 Map of the Study Area

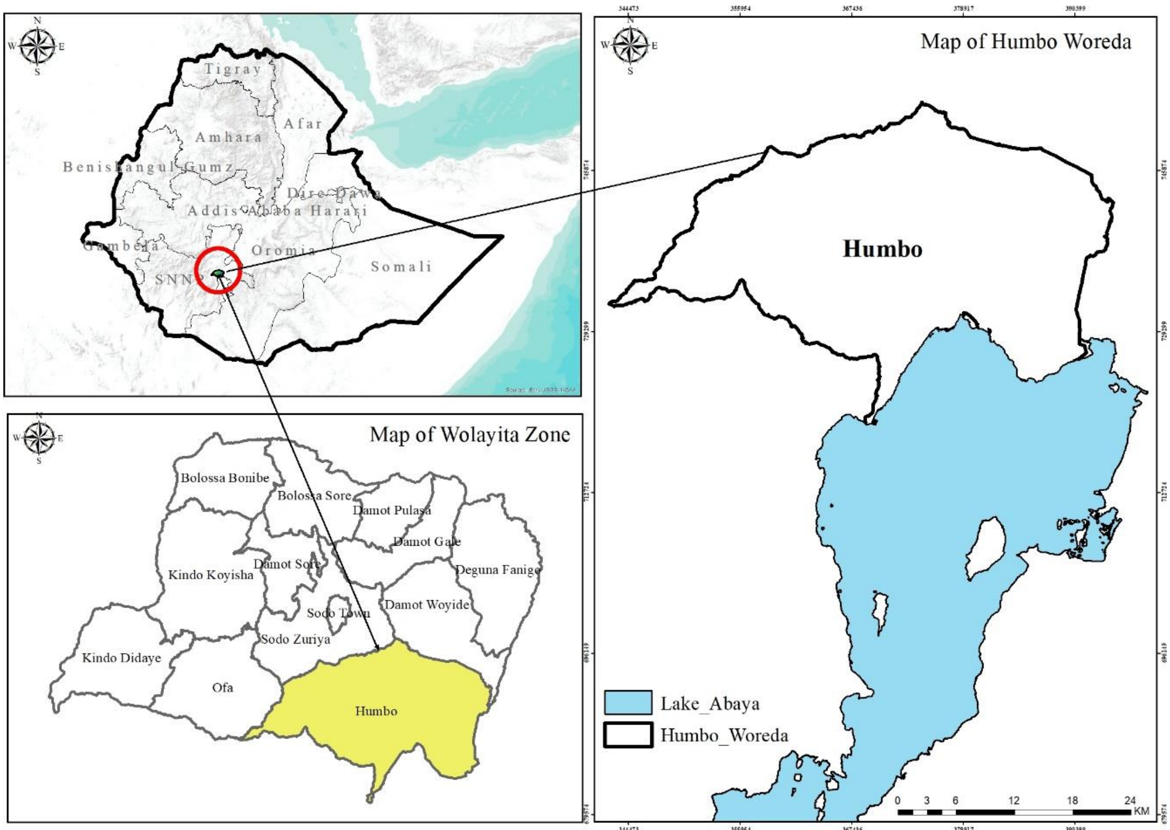

Figure 3.1 Map of the Study Area

3.1.1 Topography

The land escape is characterized by hilly terrain traversed by large plains, valleys and gorges. With regard to altitude, the largest mountain in the district is Solko Mountain which has a height of 2335m.a.s.l and the lowest area in the district is found in the south east along Lake Abaya, the largest rift valley lake, where altitude is less than 1100m.a.s.l (Fekadu 2014).

3.1.2 Agro-ecology and Climate

Agro-climatic zones, 11.11% of the Woreda falls under highland (Dega), 28% falls under mid-highland (Woina-Dega) and the remaining 61% falls under lowland (Kolla). Mean annual temperature of the Woreda is 22ºC and mean annual rainfall is 1123.15mm.

3.1.3 Vegetation Cover

The vegetation categories of the project area include Ethiopian montane grassland and woodland and Ethiopian montane forest (CDM Project, 2009).

3.1.4 Geology and Soils

The geologic formations of the Woreda belong to the Precambrian rock formation overlain by sedimentary rocks and volcanic ashes. The soils of the Woreda are mainly brownish red predominated by clay soil types.

3.1.5 Agriculture

According to the study conducted by Tadele Labiso (2021), the primary crops cultivated in the abaya lake sub-Catchment include maize, sweet potato, teff, haricot beans, coffee, cotton, and peas. Majority of the population in the woreda is primarily engaged in agriculture, typically managing a landholding size of about 0.25 hectares. Consequently, subsistence farming serves as the main source of livelihood for the community (Tadele L., 2021).

3.2 Data Sources/Datasets

In this study, several datasets are used, including satellite imagery data, topographic data, meteorological data, land use land Cover data and Land management data. These datasets are described in detail in the subsequent section

3.2.1 Satellite Imagery Data

Landsat imagery of Abaya Lake sub-Catchment with a spatial resolution of 30m was downloaded from the USGS website and preprocessed using ERDAS Imagine software prior to analysis. This preprocessing involved several critical steps, including geometric correction and atmospheric correction, to ensure the accuracy and reliability of the data.

3.2.2. Climate Data

Rainfall data were collected from the National Metrological Agency located nearby the Abaya Lake sub basin and IDW method of Interpolation were applied to estimate rainfall erosivity factor for the study area using ArcGIS Spatial Analysis Tool. The annual amounts of precipitation for the stations were collected over years by the National Metrological Agency. The majority of these mean annual precipitations were derived from more than 10 years of precipitation data.

3.2.3. Soil Data

Soil data for the study area will be obtained from the FAO Soil Map of Ethiopia (1986) and utilized to analyze the soil erodibility factor (K). The soil map is provided in a polygon format, which facilitates detailed spatial analysis. To create the soil feature map specific to the study area, the FAO soil map will be clipped to the boundaries of the study area. Following this, erodibility values (K factors) will be assigned to each soil type based on their corresponding colors, as indicated by Hurni (1985).

3.2.4 Topographic Data

A digital elevation model (DEM) is a digital model or 3D representation of a terrain's surface, created from terrain elevation data. In essence, DEMs serve as digital representations of cartographic information, crucial for various applications in Geographic Information Systems (GIS).

The accuracy of soil erosion estimates is highly sensitive to the resolution of DEMs. Lower resolution DEMs (e.g., 30 m) may not capture fine-scale topographic details, leading to inaccuracies in slope calculations and, consequently, in erosion predictions. Studies have shown that higher resolution DEMs provide more realistic slope representations, which are critical for accurate erosion modeling (Romshoo SA et al, 2021).

Therefore, for this study, resampled and corrected DEM with 12.5m resolution data was downloaded from NASA earth data website and used.

3.2.5 Land Use and land cover Data

Multi-temporal satellite imagery from the years 2003, 2015, and 2025 was imported into ERDAS image processing software for analysis. The raw images were then undergone pre-processing and enhancement to improve their quality. Subsequently, GIS software was utilized to classify the images into different Land Use Land Cover (LULC) classes using machine learning techniques. For this study the researcher utilized a random forest classifier. The classified images then served as the basis for extracting information on land cover conditions and quantifying the C-factor values over the past three decades through multi-temporal GIS analysis.

3.3 Remote Sensing Data Analysis

3.3.1 Image Preprocessing

Image preprocessing like geometric correction and atmospheric correction are conducted to enhance the satellite image quality using ERDAS IMAGIN image processing software.

Landsat ETM+ with 30-m resolution digital satellite imagery of the year 2003, 2015 and

2025 were used to generate thematic maps of the sub-watershed. The multitemporal Landsat images used in this study are indicated in table 3.2.

Table 3.1 Description of Multi-temporal images used.

Image	Path/Row	Acquisition Date	Spatial Resolution(m)
Landsat 7 ETM C2L	169/055	02/20/2003	30m*30m
Landsat 8 OLI/C2L1	169/055	02/13/2015	30m*30m
Landsat 8 OLI/C2L1	169/055	02/08/2025	30m*30m

3.3.2 Training Site Selection

In this research, the selection of training sites for the Random Forest classifier has adopted a systematic methodology. The study area was first be defined to include a variety of land cover types. A minimum of 200 ground truth points was collected through field surveys and existing datasets to ensure a robust dataset that captures the variability of land cover across Abaya Lake Sub Basin.

To achieve adequate representation of all classes, ground truth points was strategically distributed across the region, covering diverse categories such as agricultural fields, forests, urban areas, and water bodies. A systematic sampling approach was then employed, utilizing a grid overlay on the study area to ensure even coverage and minimize bias in point selection. Each ground truth points then undergo verification using high-resolution satellite imagery (Google Earth). This verification process is crucial for confirming the accuracy of land cover classifications and enhancing the reliability of the training dataset.

Additionally, ground truth data collection was conducted across different seasons to account for seasonal variations in land cover. This temporal consideration ensures that the training dataset accurately reflects the dynamic nature of land use in the area.

Once the ground truth points were collected and verified, they were organized into a structured dataset with relevant attributes and labels, which was then integrated into GIS software for spatial analysis. The Random Forest classifier was trained using this dataset, with parameters optimized to enhance accuracy.

3.3.3 LULC Classification

Satellite images from different time periods (2003,2015 and 2025) were downloaded from the USGS website and utilized for the Land Use Land Cover (LULC) assessment of the sub-catchment. This multi-temporal raw satellite data was imported into ERDAS Imagine image processing software, where various image rectification, enhancement, and classification techniques was applied to the raw images. The LULC classification then conducted using GIS machine learning tools, specifically, using Random Forest classifier. Ultimately, land cover and C-factor maps was generated for the three study periods (2003, 2015, and 2024) using the Random Forest classifier within the GIS environment.

3.3.3.1 Accuracy Assessment

The accuracy of land cover classification was evaluated using an error matrix, which illustrates the relationship between the classified data and reference data obtained from filled and Google Earth imagery. This reference data provided a reliable basis for assessing classification accuracy. A set of independent reference points were established to evaluate the classification, ensuring that these points are distinct from those used in the land cover class assignment. In total, 100 reference points were selected within the watershed and verified against the Google Earth imagery and filled collected data. Then Error matrices are constructed to assess the quality of the classification. Overall accuracy was calculated by dividing the total number of correctly classified pixels (the sum of the diagonal elements in the error matrix) by the total number of pixels in the matrix:

$$\text{Overall Accuracy} = \frac{\text{Total Correctly Classified Pixels}}{\text{Total Pixels in Matrix}}$$

Producer’s accuracy was determined to reflect the probability that a reference pixel is classified correctly. This metric was calculated by dividing the number of correctly classified pixels in a specific category by the total number of reference pixels for that category. User’s accuracy will also be assessed to evaluate the probability that a pixel classified in a specific category accurately represents that class on the ground (Congalton, 1991). User accuracy was computed by using the following equation.

$$\text{User s Accuracy} = \frac{\text{Correctly Classified Pixels in Category}}{\text{Total Pixels in Classified Image for Category}}$$

The Kappa coefficient was also utilized to quantify classification accuracy, measuring the proportionate reduction in error generated by the classification compared to random classification using the following equation.

$$\text{Kappa} = \frac{(\text{Po}-\text{Pe})}{(1-\text{Pe})}$$

where Po is the observed agreement and Pe is the expected agreement by chance (Congalton, 1991).

Kappa statistics and error matrices are sufficient for model validation due to their ability to provide a comprehensive assessment of classification accuracy. The kappa coefficient measures the agreement between predicted classifications and actual truth values, offering a more nuanced view than overall accuracy alone, which can be misleading in imbalanced datasets. A kappa value of 1 indicates perfect agreement, while a value of 0 signifies no agreement, thus allowing researchers to quantify the reliability of their classification results (McHugh ML, 2012). Error matrices complement this by detailing the number of true positives, false positives, true negatives, and false negatives, enabling the identification of specific errors such as commission and omission rates. Together, these tools not only validate model performance but also highlight areas for improvement, making them essential for effective accuracy assessment in various applications.

Accordingly, Table below shows the classification accuracy.

Table: 3.2 Land Cover Classification Accuracy confusion metrics

Class Name	BU	Ag	Wat	BL	For	Ens	WL	ShL	FL	WetL	GL	Row Total
BU	83	5	1	3	1	1	2	1	1	1	1	100
Ag	6	82	2	2	1	2	1	1	1	1	1	100
Wat	1	2	89	1	1	0	1	1	2	1	1	100
BL	5	3	1	83	2	1	1	1	1	1	1	100
Fore	1	4	1	2	84	2	1	2	1	1	1	100
Enset	1	6	1	1	2	83	1	2	1	1	1	100
WL	2	1	1	1	1	2	84	5	1	1	1	100
ShL	1	2	1	1	2	5	1	84	1	1	1	100
FL	1	5	2	1	1	1	1	2	84	1	1	100
WetL	1	1	1	2	1	1	1	1	5	85	1	100
GL	1	3	1	1	1	1	1	1	1	1	88	100
Column Total	100	100	100	100	100	100	100	100	100	100	100	**1100**

Based on the above confusion matrices, the overall accuracy is calculated to be 84.5% and its Kappa Coefficient (κκ) is found to be 0.835.

3.4 Methods of Spatial Data Generation

3.4.1 Random Forest Classifier

Random Forest (RF) is a versatile non-parametric ensemble machine learning algorithm developed by Breiman, widely recognized for its effectiveness in addressing various environmental challenges, including water resource management and natural hazard mitigation. This algorithm is particularly adept at processing diverse data types, such as satellite imagery and numerical datasets, making it highly suitable for Land Use and Land Cover (LULC) classification and the extraction of RUSLE (Revised Universal Soil Loss Equation) parameters (Breiman, 2001; Zhang et al., 2018).

As an ensemble learning method, RF constructs multiple decision trees and aggregates their outputs to enhance regression and classification accuracy. Key parameters for setting up an RF model include the number of trees ('n-tree') and the number of features considered at each split ('m-try'). Each decision tree contributes a vote towards the final classification outcome, with the majority vote determining the predicted class (Liaw & Wiener, 2002).

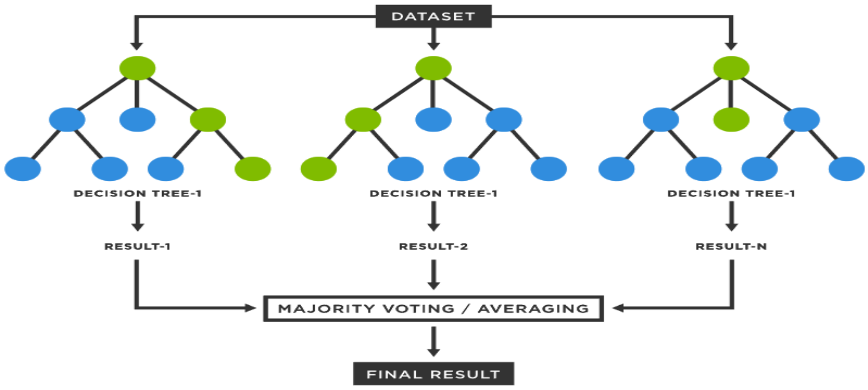

Figure 3.2 RF-Algorism

Recent studies have highlighted the effectiveness of RF in LULC classification within remote sensing applications, often achieving high accuracy rates, such as Kappa coefficients exceeding 0.84 (Gomez et al., 2020; Rojas et al., 2021).

The performance of RF improves with an increased number of trees; however, Breiman cautioned that using more trees than necessary can lead to inefficiencies without significantly enhancing model performance. In one study by Feng et al. (2018), 200 decision trees were employed, yielding accurate results. In this research the 'Random Forest' classifier in ArcGIS/QGIS was applied to classify LULC and extract RUSLE parameters, employing 200 decision trees with three input features as recommended by previous studies. This approach aligns with findings that emphasize RF's effectiveness in LULC classification tasks using various remote sensing datasets (Zhang et al., 2018).

3.4.2 RUSLE-Model Description

The Revised Universal Soil Loss Equation (RUSLE) is an empirical erosion model recognized as a standard method to calculate the average risk of erosion on arable land. This model was developed as an improved version of the original Universal Soil Loss Equation (USLE), addressing the limitations of its predecessor by incorporating more accurate and less data-intensive methodologies (Renard et al., 1997).

While RUSLE retains the empirical principles and fundamental structure of the USLE, it introduces significant modifications that enhance its applicability, particularly in developing countries. These enhancements include new term values, correction factors, algorithms for calculating parameters, and refined approaches to slope morphology. RUSLE provides improved methods for estimating key factors such as rainfall erosivity (R), soil erodibility (K), slope length and steepness (LS), land cover management (C), and conservation practice (P) factors (Wischmeier & Smith,1978; Bhadur, 2009; Ganasri & Ramesh, 2016).

In this study, the RUSLE model was executed in conjunction with raster-based Geographic Information Systems (GIS) to predict erosion potential on a cell-by-cell basis (Millward & Mersey, 1999).

The analysis utilizes grid cells of 12.5m × 12.5m to compute the physical characteristics influencing soil erosion processes, including slope, land use, and soil type across different areas of the watershed. This methodology was crucial for establishing a uniform spatial analysis environment suitable for GIS modeling (Wischmeier & Smith, 1978; Bhadur, 2009).

The RUSLE model is formulated as an equation that represents the primary factors controlling soil erosion: climate, soil characteristics, topography, and land cover management. The equation is expressed as:

$A = R \times K \times LS \times C \times P$………………………………...……..…..………………….… Eq1.

Where **A** is the annual soil loss, "**R**" is runoff erosivity, "**K**" is soil erodibility, "**L**" is slope length, "**S**" is slope steepness, "**C**" is cover-management factor, and "**P**" is support practice factor. See the general flow diagram below.

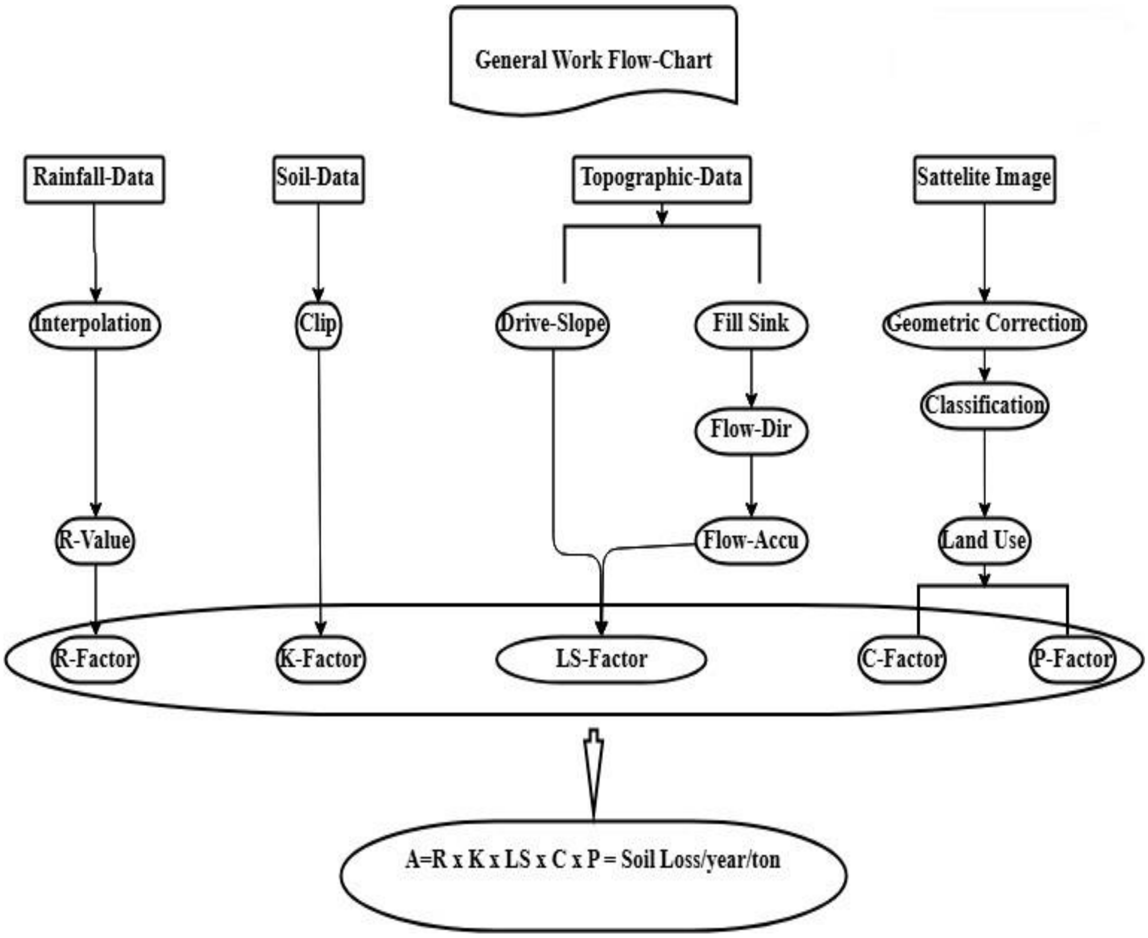

Figure 3.3 RUSLE-General Work Flow Chart

The details of the work flow and how each soil erosion factors are derived explained in the below section.

3.4.2.1 Rainfall Erosivity (R) factor

Rainfall erosivity (R) is one of the critical factors in assessing the potential for soil erosion caused by rainfall events. It quantifies the potential of a rain to induce erosion, defined as the product of the total energy of a rainstorm (E) and the maximum 30-minute intensity (I30), expressed as EI30. The annual erosivity can be estimated by summing the rainfall erosivity of individual erosive storms throughout the year or season (Yin et al., 2023; Borrelli et al., 2021).

R-factor calculation requires, long-term rainfall data, which may not be readily available for the entire sub basin. To address this limitation, relationships between the rainfall erosivity index and annual rainfall was established using data from nearby meteorological observatories. The data was then interpolated to estimate rainfall within the study area using ArcGIS 10's Spatial Analysis Tool. For this study, a time series of 30 years of rainfall data were utilized to estimate the "R" value for the years 2003, 2015, and 2025. After obtaining the interpolated rainfall data, the R-factor within the study area were calculated based on a model developed by Hurni (1985), specifically tailored for Ethiopian conditions, as it is represented by the equation:

$R = -8.12+(0.562\times P)$ ……………………………………………………………………Eq2

where P is the mean annual rainfall in millimeters (Hurni, 1985; Borrelli et al., 2021).

In order to compute "R" factor for the sub basin, seven metrological stations i.e (Belle, Bedesa,Gessuba, Mayokote, Wajifo, Humbo Tebela and Dinka) with mean annual rainfall of 30 years were used but for some stations, because of lack of available data, mean annual rain fall of less than ten years were used. The three tables below show, the name, location, mean annual precipitation and erosivity value of each of the metrological stations used for "R" factor generation for the study periods 2003, 2015 and 2025. Table 3.3 Mean annual precipitation and Erosivity value of the year 2003 for rain fall stations.

Table 3.3 Mean annual precipitation and Erosivity value of the year 2003

ID	Station	Elevation	Long	lat	RF-Mean	R-Factor
1	Dinke	1596	37.42167	6.447222	1299	721.92
2	Mayokote	2121	37.85319	6.885833	1602	892.20
3	Wajifo	1230	37.74167	6.455833	928	513.42
4	Bedessa	1711	40.7712	8.90833	1066	590.97
5	Gessuba	1552	37.56278	6.729167	1048	580.86
6	Humbo Tebela	1618	37.76556	6.703056	1134	629.19

Source: ENMA (2025) * duration of data used 1980-2003

Table 3.4 Mean annual precipitation and Erosivity value of the year 2015

ID	Station	Elevation	Long	lat	RF-Mean	R-Factor
1	Humbo Tebela	1618	37.76556	6.7	1129.54	626.68
2	Gessuba	1552	37.56278	6.73	1080.68	599.22
3	Bedessa	1711	40.7712	8.91	1079.709	598.67
4	Wajifo	1230	37.74167	6.46	1031.07	571.34
5	Mayokote	2121	37.85319	6.89	1542.152	858.57
6	Dinke	1596	37.42167	6.45	1298.337	721.55
7	Belle	1596	37.42167	6.45	976.2879	540.55

Source: ENMA (2025) * duration of data used 1980-2015

Table 3.5 Mean annual precipitation and Erosivity value of the year 2025

ID	Station	Elevation	Long	lat	RF-Mean	R-Factor
1	Humbo Tebela	1618	37.76556	6.7	1094.996	607.28
2	Belle	2422	40.00167	7.73	980.6569	543.01
3	Gessuba	1552	37.56278	6.73	1065.286	590.57
4	Bedessa	1711	40.7712	8.91	1075.025	596.05
5	Wajifo	1230	37.74167	6.46	1054.228	584.36
6	Mayokote	2121	37.85319	6.89	1512.513	841.91
7	Dinke	1596	37.42167	6.45	1279.214	710.79

Source: ENMA (2025) * duration of data used 1980-2024

After having the average rainfall data of each metrological station, Invers Distance Weight method of interpolation using ArcGIS spatial analyst tool was used to generate an estimated surface from these scattered set of point data into surface. In Figure 3.4 below, the spatial distribution of the computed rainfall erosivity for the year 2003, 2015 and 2025 is given.

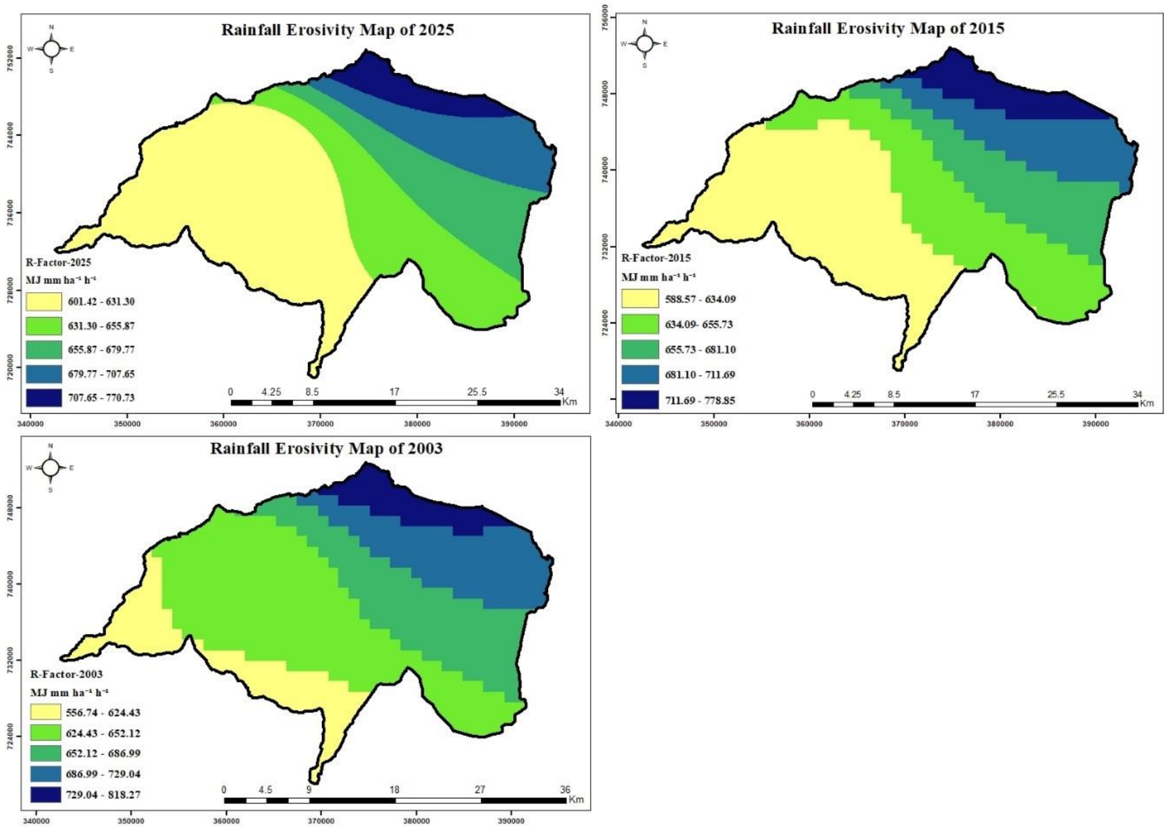

Figure 3.4 Rainfall Erosivity Map

Recent research finding conducted based on large scale modeling i.e. General Circulation Models (GCMs) and Representative Concentration pathways (RCPs) indicated that, global rainfall erosivity is expected to rise by 26.2% to 28.8% by 2050 and 27% to 34.3% by 2027 relative to the level in 2010. And this rise in rainfall erosivity is identified as the main driver behind the projected 30 to 66% rise in global soil erosion rate by 2070, assuming there will be no major change in land management practices (Panagos, et'al;2022).

As shown in the above figure, the spatial distribution of the computed rainfall erosivity for the year 2003 ranges from 588.57 to 778.86 MJ mm ha^{-1} h^{-1} y^{-1} with the average value 654.76MJ mm ha^{-1} h^{-1} y^{-1} , while it ranges from 556.74 to 818.28 MJ mm ha^{-1} h^{-1} y^{-1} with the average value 645.23 MJ mm ha^{-1} h^{-1} y^{-1} and from 601.43 to 770.73MJ mm ha^{-1} h^{-1} y^{-1}, with the average value of 639.28 MJ mm ha^{-1} h^{-1} y^{-1} for the year 2015 and 2025 respectively. The data also shows a general decline in rain fall erosivity from the year 2003 to 2025.

3.4.2.2 Soil Erodibility (K) factor

The Soil Erodibility (K) factor represents the susceptibility of soil to erosion and the rate of runoff, which are influenced by various soil properties, including texture, organic matter, structure, and permeability (Efe et al., 2008; Titmarsh, 2018).

The K factor reflects how easily soil can be detached by splash during rainfall or by surface flow, indicating the change in soil due to applied external forces (Dumas & Printemps, 2010). It is related to the integrated effects of rainfall, runoff, and infiltration on soil loss, accounting for the influences of soil properties during storm events in upland areas (Lu et al., 2004).

A simpler method for predicting the K factor was presented by Wischmeier and Smith (1978), which incorporates particle size distribution, organic matter content, soil structure, and profile permeability. The USLE monograph estimates erodibility as follows:

$K=2.1\cdot M1.14\cdot 106\cdot(12-MO) +0.032\cdot(b-2) + 0.025\cdot(c-3)$ Eq 3…………..………… Eq 3

where M is the percentage of silt plus very fine sand (100 minus percentage clay), MO is the percent organic matter content, b is the soil structure code, and c is the soil permeability rating (Wischmeier & Smith, 1978; Borrelli et al., 2021).

However, due to challenges in obtaining local parameters for this equation and constraints related to time and cost for analyzing soil samples in the study area, this research has adopted the erodibility factor (K) by Tadesse et al., (2021); Wagari & Tamiru, (2021), for Ethiopian conditions. This approach will utilize soil color as an indicator of erodibility to determine K values. Soil data was obtained from the digital soil map of Ethiopia (FAO, 1986), with soil characteristics clipped from this map. The K value for each soil type the was assigned based on their color as indicated by Hurni (1985).

The soils of the study area contain seven distinctive erodibility values. Table 3.6 below shows the detail of soil type, soil color and erodibility factor value in the watershed. Accordingly, soil erodibility in the sub basin ranges from 0.1 to 0.25 $ton\cdot ha\cdot hr\cdot ha^{-1}\cdot MJ^{-1}\cdot mm^{-1}$. Higher values of soil erodibility indicate its higher susceptibility to erosion.

Table 3.6 Soil Erodibility Factor (K)

#	Soil Type	Soil Color	K Factor
1	Chromic Luvisols	Reddish-brown to yellowish	0.25
2	Chromic Vertisols	Dark grey to black	0.18
3	Eutric Fluvisols	Greyish to brown	0.22
4	Eutric Nitosols	Dark reddish-brown	0.15
5	Eutric Regosols	Light brown to grey	0.2
6	Leptosols	Pale brown to grey	0.13
7	Vertic Andosols	Dark brown to black	0.1

Source: *Tadesse et al., 2021; Wagari & Tamiru, 2021*

NB Water and Ston cover area identified as no color with 0 K factor value

The basic soil data set was found in vector format. After changing the vector format in to grid, the grid data set was reclassified based on K-value of each soil class in ArcGIS 10. Figure 3.5 below shows, raster map of soil erodibility factor "k" in the sub-Catchment.

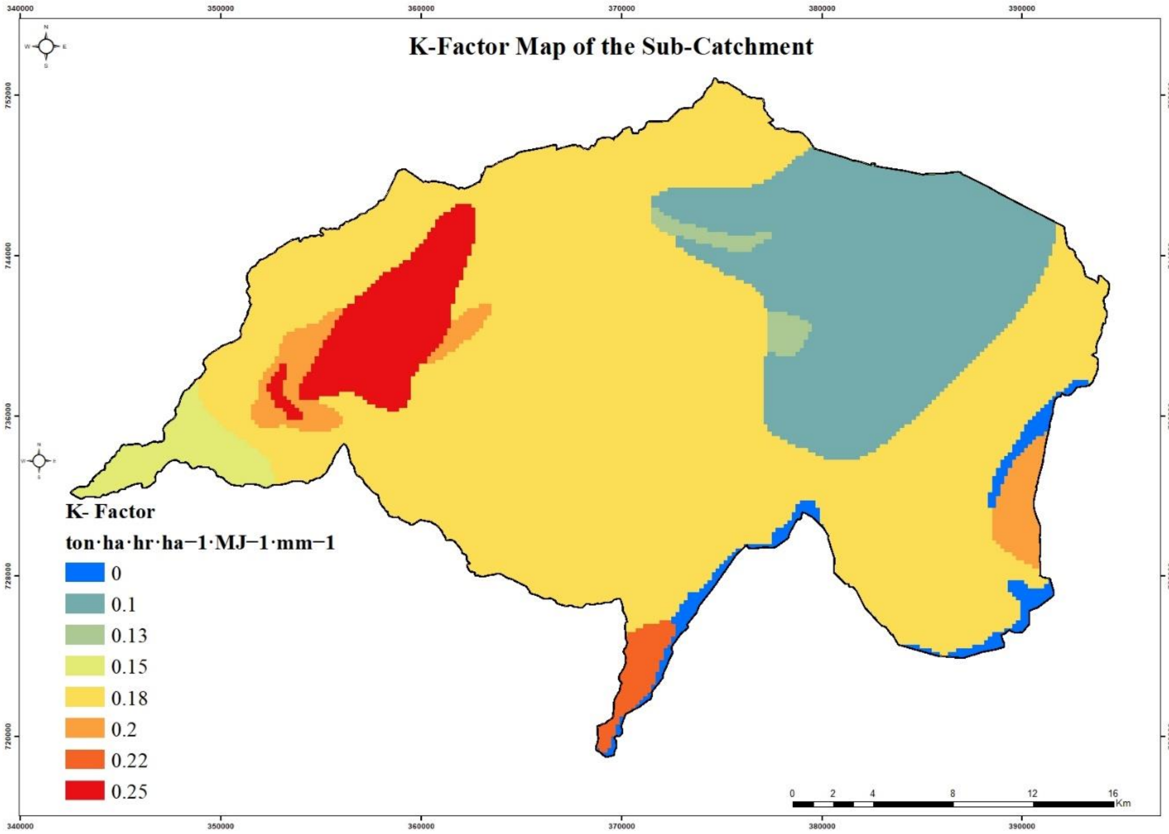

Figure 3.5 K Factor Map

Based on the soil map, Chromic Luvisols, with erodibility factor 0.25ton·ha·hr·ha−1·MJ−1·mm−1, covers an area of 4,436 hectare of the of the watershed which is about 5% of the total land area, while Chromic Vertosols with a soil erodibility factor of 0.17ton·ha·hr·ha−1·MJ−1·mm cover vast majority of the Sub-catchment accounting around 66%.

3.4.2.3 Slope Length and Steepness Factor (LS)

The L and S factors in the Revised Universal Soil Loss Equation (RUSLE) reflect the influence of topography on soil erosion. Increases in slope length and slope steepness significantly enhance overland flow velocities, leading to higher erosion rates (Dai et al., 2022; Haan et al., 1994). Research indicates that gross soil loss is considerably more sensitive to changes in slope steepness than to changes in slope length, emphasizing the critical role of the S factor in erosion dynamics (McCool et al., 2021). Slope length is broadly defined as the distance from the point of origin of overland flow to the point where either the slope gradient decreases sufficiently for deposition to begin or where flow is concentrated into a defined channel (Wischmeier & Smith, 1978). The specific effects of topography on soil erosion will be estimated using the dimensionless LS factor, which is the product of the slope length (L) and slope steepness (S) components converging onto a point of interest, such as a farm field or a cell on a GIS raster grid. To derive the LS factor, a Digital Elevation Model (DEM) with a resolution of 12.5m was processed after appropriately clipped by the study area. The LS factor grid was estimated using equations proposed by Moore and Burch (1986) and Engel (2005), which have been validated through recent studies demonstrating their applicability in diverse landscapes (Bagegnehu Bekele & Yenealem Gemi, 2021; Azedou et al., 2023).

LS= ((flowacc * cell resolution) ^0.4)) /22.1 * ((sin (slope in radians)) ^1.4)/0.09…Eq4

Where LS represents the slope steepness-length factor, and each cell size is 12.5 m by 12.5 m in contributing area.

Using the Spatial Analyst Extension in ArcGIS, the slope of the catchment area was derived from the DEM. Any sinks present in the DEM were identified and filled to ensure accurate flow modeling. The filled DEM then used as input to determine Flow Direction, which then subsequently be used for deriving Flow Accumulation.

Finally, the LS factor was computed using Raster Calculator in ArcGIS based on flow accumulation and slope steepness.

Figure 3.6 below shows the combined LS factor in the watershed which is calculated based on flow accumulation and slope. Accordingly, LS factor in the watershed ranges from 0 to 13.2819, with the mean value for the entire watershed at approximately **0**.0047 and a standard deviation of 0.0377.

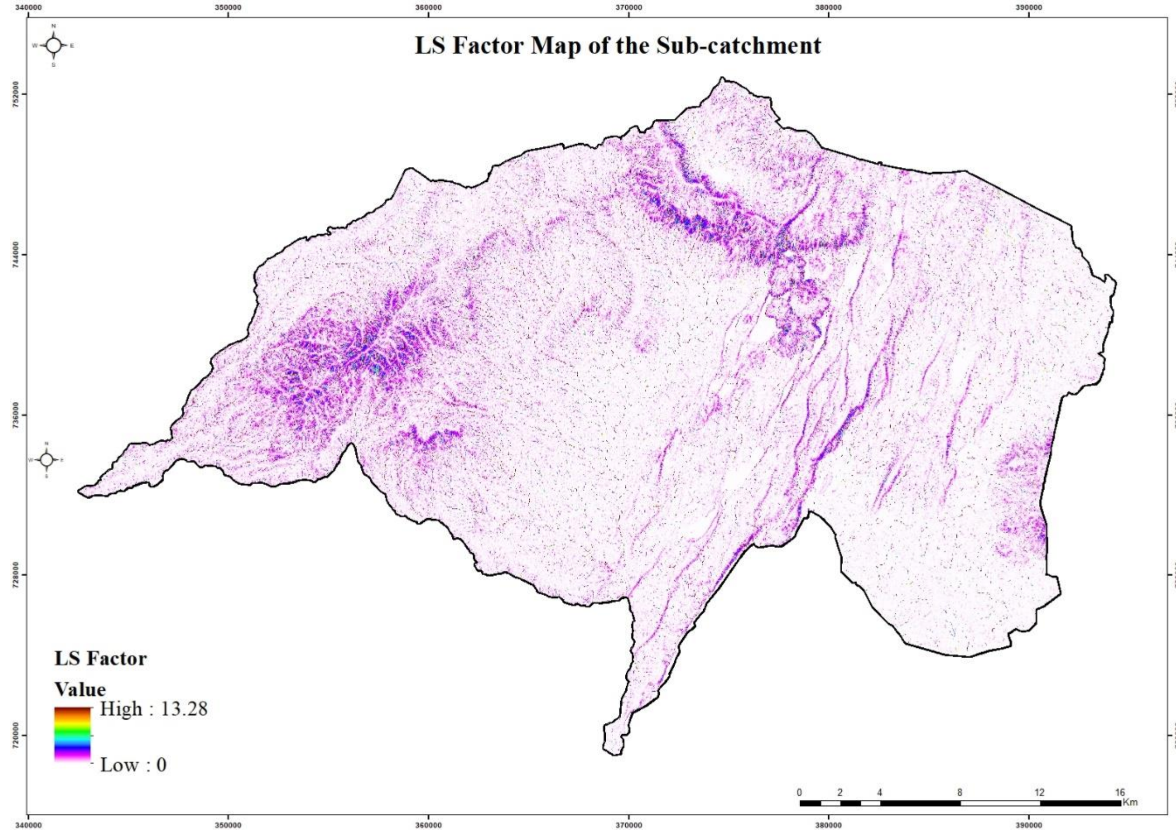

Figure 3.6 LS Factor Map

3.4.2.4 Cover Management Factor (C)

The Cover Management Factor (C) represent the effect of vegetation cover and management practice on soil erosion in agricultural and non-agricultural settings.

Recent research indicates that the C factor, along with slope steepness and length factors, is particularly sensitive to soil loss, making it a crucial component in soil erosion modeling (Han et al., 2020; Ferreira & Panagopoulos, 2014). The C factor reflects how different land use practices, such as crop type, tillage methods, and vegetation cover, influence soil erosion rates.

In this study, Landsat imagery from the years 2003, 2015, and 2025 with a resolution of 30 m was utilized for land use and land cover classification. Field observations and ground truth data collection and Google earth were employed to support the classification process and enhance accuracy.

After the classification is done, the raster layer was converted into vector layer and "C-factor" value was assigned for each land use land cover unit based on Hurni (1985), Nyssen et al. (2002), Wagari & Tamiru (2021), Tadesse et al. (2021) which is adopted for Ethiopian condition.

Accordingly, land Sat Image of 2003,2015 and 2025 with 30-m resolution was interpreted in to ten class i.e. Agricultural Land, Enset (False Banana), Grass Land, forest, Shrub/Bush, Wood Land, Bare Land, Built up (Dense), wet Land, Flooded area and Large-Scale Irrigation.

After the classification was done Agricultural Land and large-scale irrigation was merged in to one class since the researcher only want to focus and work on Land Use and Land Cover type rather than land use unit, and then based on the classification of the 2025 land sat image the rest of the study period were classified i.e. 2003, and 2015.

The land use land cover map of the three study periods is presented in the figure 3.7 shown below.

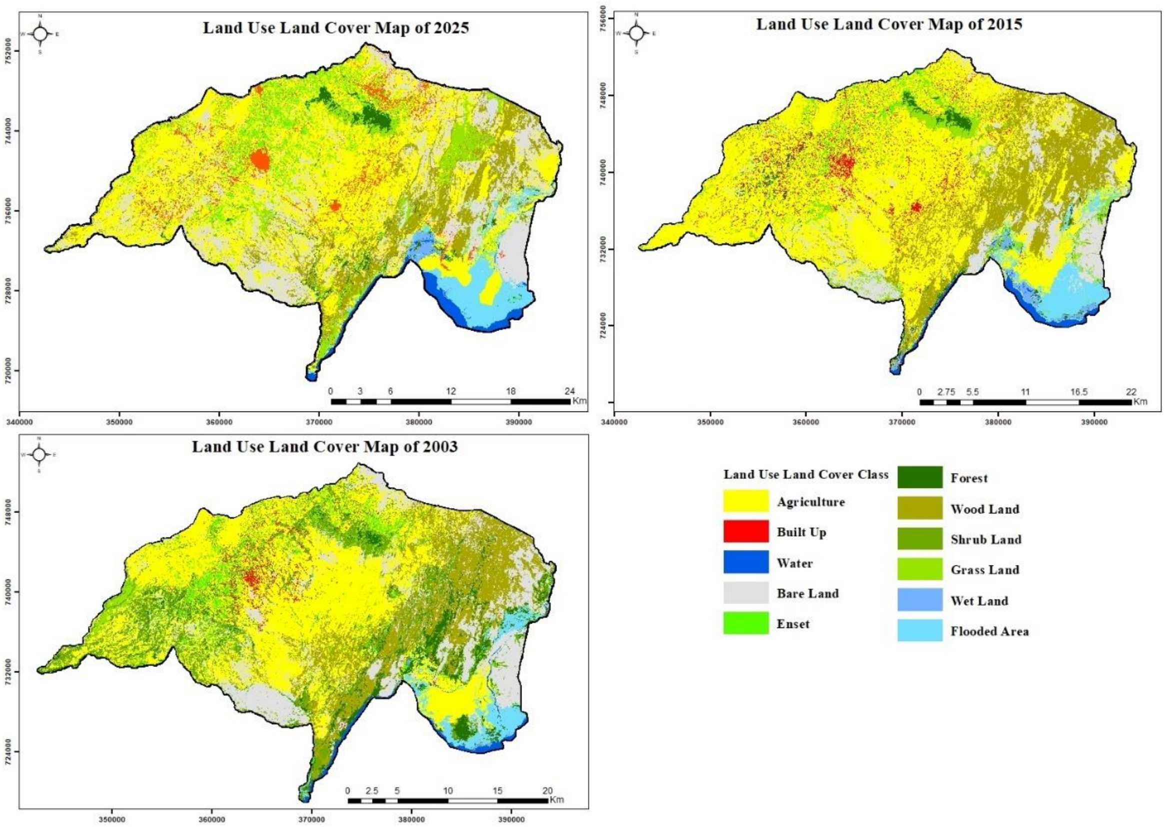

Figure 3.7 Land Use Land Cover Map

Table 3.7 below shows the different class of the land use land cover type in 2003, 2015 and 2025.

Table 3.7 Land Use Land Cover for 2003,2015 & 2025

Land Cover Type	**Year-2003**		**Year-2015**		**Year-2025**	
	Area (Ha)	**2003%**	**2015-Area (Ha)**	**2015%**	**2025-Area (Ha)**	**2025%**
Built Up	1158.03	1.3%	3324.54	3.9%	4044.26	5%
Agriculture	32270.79	37.5%	45121.54	52.4%	37948.19	44%
Water	704.92	0.8%	957.02	1.1%	1620.28	1.9%
Bare Land	13569.75	15.8%	9369.03	10.9%	17222.56	20.0%
Forest	4459.38	5.2%	1447.65	1.7%	1824.13	2.1%
Enset	3003.18	3.5%	3380.24	3.9%	4623.35	5.4%
Wood Land	13354.17	15.5%	14767.71	17.2%	9539.3	11.1%
Shrub Land	11953.15	13.9%	3260.9	3.8%	4664.29	5.4%
Flooded Land	2736.12	3.2%	3437.49	4.0%	4035.21	4.7%
Wet Land	155.53	0.2%	979.86	1.1%	524.41	0.6%
Grass Land	2680.96	3.1%	*	*	*	*
Total Area	**86045.98**		**86,045.98**		**86045.98**	

Based on the identified land Use Land cover class, RUSLE -C factor value was assigned as show in the table below.

Table 3.8 C-Factor

#	Land Cover Type	RUSLE C-Factor
1	Bare Land	1
2	Agriculture/Cultivated Land	0.15
3	Built-up Area/Urban	0.15
4	Shrub Land	0.05
5	Grass Land	0.01
6	Enset	0.02
7	Wood Land	0.06
8	Wet Land	0.01
9	Forest	0.01
10	Flooded Area	0.35
11	Water	0

Source: *Nyssen et al. (2002), Wagari & Tamiru (2021), Tadesse et al. (2021), Hurni (1985), Anteneh and Biru (2021), Tiruneh and Ayalew (2015)*

As indicated in the table above, bare land has the highest c-factor value “1,” implying high susceptibility to soil erosion, followed by flooded areas, agricultural land, and built-up areas, with a c-factor values “0.35”, “0.15” and “0.15” respectively.

Additionally, Shrub land and wood land soil susceptibility factor ranges between “0.05” and “0.06”, while water, wet land, forest, Grass land and Enset are assigned a c-factor value of “0”, “0.01”, “0.01” and “0.02”. Based on the above table, c-factor maps of the years 2003, 2015 and 2025 are presented in figure 3.8 below.

Figure 3.8 below shows the spatial distribution in C - factor value in the Sub-catchment over time

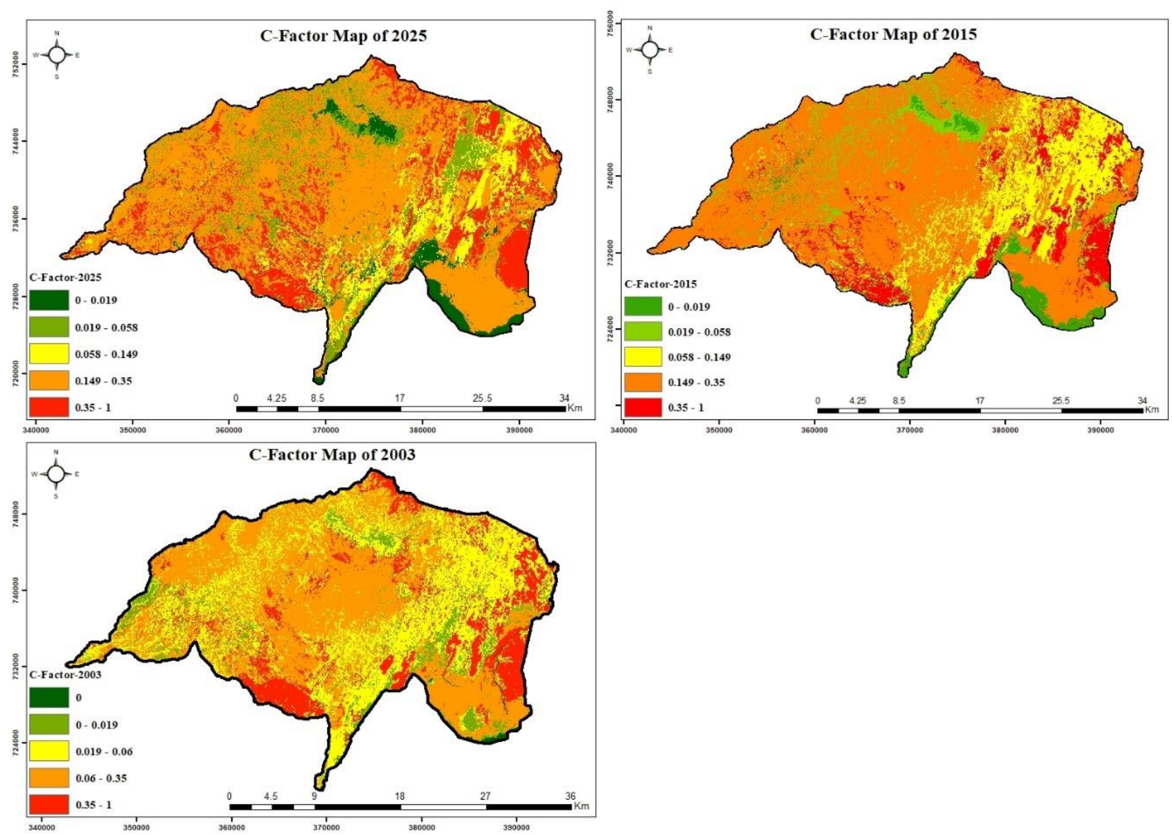

Figure 3.8 C-Factor Map

3.4.2.5 Conservation Practice Factor (P)

The Conservation Practice Factor (P), also known as the support factor, represents the ratio of soil loss after implementing specific conservation practices compared to the corresponding soil loss without these practices. This factor reflects the effectiveness of soil and water conservation practices in reducing erosion (Ouadja et al., 2022; Iticha & Takele, 2018). The P factor ranges from 0 to 1, where lower values indicate more effective conservation practices. In this study, due to difficulties in obtaining reliable information on conservation practices employed by farmers and the likelihood of lacking permanent management strategies, the researcher will utilize P-values suggested by Bewket and Teferi (2009), Wischmeier and Smith (1978), and Shi et al. (2002).

Recent literature emphasizes the importance of accurately determining P-values based on local conditions and land use types. These values typically consider two types of land use: agricultural and non-agricultural, along with variations in slope. Agricultural lands was classified into different slope categories, with corresponding P-values assigned; all non-agricultural lands then assigned a P-value of 1.00 (Fayas et al., 2019; Negash et al., 2021). Recent studies have highlighted that the P-factor is crucial for understanding how different conservation practices—such as contour farming, strip cropping, and terracing—impact soil loss. Effective management practices can significantly lower the P-factor, thereby reducing soil erosion risk (Gashaw et al., 2020; Sharma et al., 2023). The assignment of P-values for each land use type was conducted using GIS techniques to ensure accurate spatial representation and facilitate better decision-making for conservation efforts. See table 3.10 below.

Table 3.9 P-value suggested by Wischmeier and Smith (1978)

Land use type	**Slope (%)**	**P-factor**
Agricultural land	0-5	0.1
	5-10	0.12
	10-20	0.14
	20-30	0.19
	30-50	0.25
	50-100	0.33
Other Land	All	1.00

Source: Wischmeier and Smith (1978)

Based on the p – value suggested by Wischmeier and Smith (1978), the sub basin was classified in to two class i.e. agricultural land and non-agricultural land. Beside this the agricultural land was again classified in to six different slope class upon which p – factor value was assigned accordingly, as shown in table 3.10, while a P – factor value “1” was assigned to all the non-agricultural land within the study area.

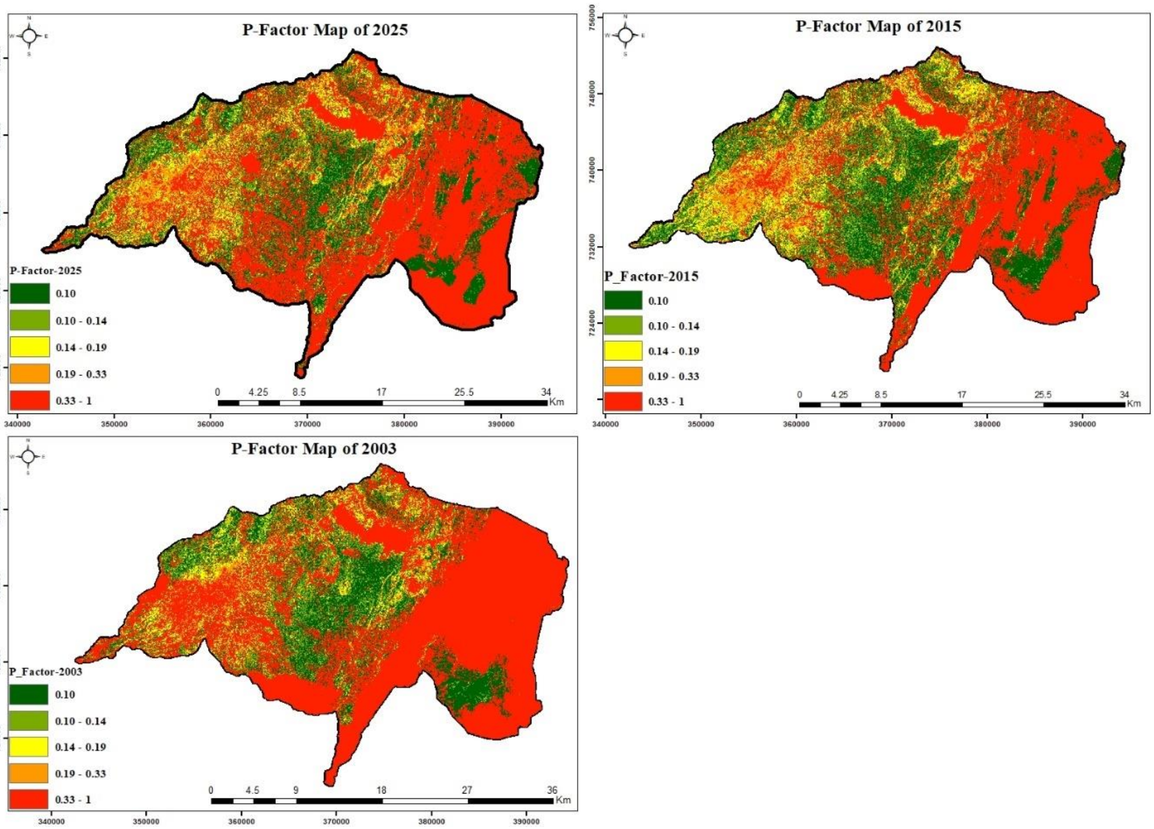

Figure 3.9 P-Factor Map

CHAPTER FOUR

4. RESULTS AND DISCUSSION

4.1 Extent and Rate of Soil Erosion in Abaya Lake Sub Basin Watershed

Based on the analysis, the total soil loss for the year 2025 was calculated to be 2.83milions.ton/hectare/year from the total area of 86,046hectar of land. To determine annual soil loss rate, a detailed cell by cell analysis of the soil loss surface was conducted. This applies multiplying the relevant RUSLE (Revised Universal Soil Loss Equation, factor values using ArcGIS 10. Based on the methodology described in equation (1).

The study also identified that, there is a significant variation in the potential annual soil loss rate as well as the average soil erosion rate distribution across the different regions in the sub-catchment. While the potential annual soil loss rate ranges from 0 to 508. 97ton.hectare/year, the average annual soil loss rate across the entire sub-catchment is calculated to be 32.84ton/hectare/year.

Beside the above, the study also revealed variation in the amount of soil erosion rate across the sub catchments. For instance, the western part of the sub basin exhibited a soil loss range from 0 to 508.9ton/hectare/year while the upper catchments, middle catchment and lower catchment showed 0.0 to 101.1, 0.0 to 80.4 and 0.0 to 64.94ton/hectare/year respectively.

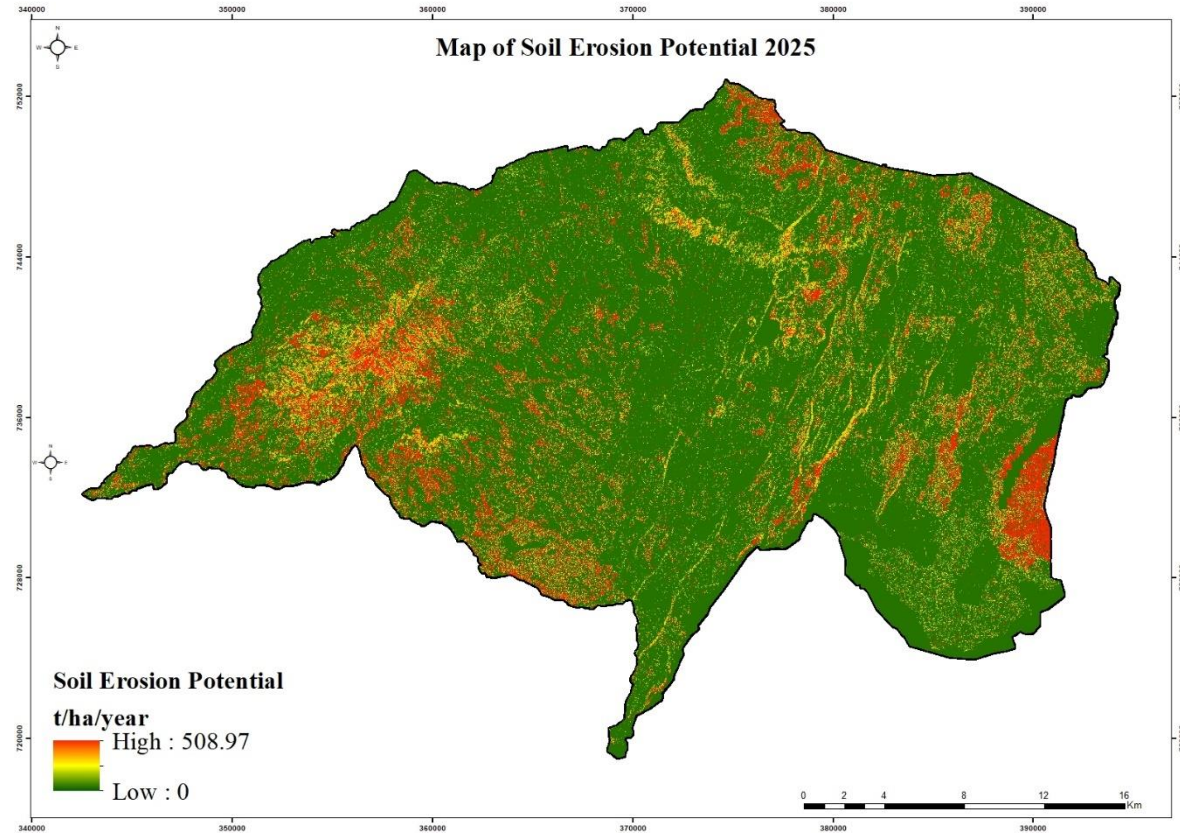

Figure 4.1 Soil Erosion Potential Map of 2025

The study conducted in the Abaya Lake sub-Catchment revealed an average annual soil loss of rate of 32.84ton/hectare/year. This finding aligns closely with the result from various other researchers across Ethiopia, reinforcing the notion that soil erosion is a widespread issue in the region. For example, a recent study by Seifu kebede and Fikadu Fufa (2023) in the Finca'aa area of Oromia reported a comparable soil loss rate of 33.3ton/hectare/year. Such consistency indicates that the soil erosion rate observed in the Abaya Lake Sub Basin are reflective of trends in other areas (Seifu et al., 2023).

Further corroborating these findings, Arega et al. (2024) assessed the upper Bilate watershed and estimated an average annual soil loss rate of 24.1tone/hectare/year, with variation ranging from 0.05 to 498.24ton/hectare/year. Similarly, Dawit Bobe et al. (2025) documented an average soil loss of 22ton/hectare/year in the Gununo watershed, highlighting a commonality in erosion rates across different regions (Dawit et al. (2025).

In More extreme cases, research by Negese et al. (2021) in the Chereti watershed identified steep slopes with soil loss rate reaching as high as 187.47tone/hectare/year and a mean annual soil loss of 38.9ton/hectare/year. Mustefa et al. (2019) also observed a significant variability in the Hanger River watershed, where soil loss rate ranged from 1 to 500ton/hectare/year, averaging 32ton/hectare annually.

Additionally, Tesfaye and Tibebe (2018) documented a mean annual oil loss of 62.98 ton/hectare/year in the Megech watershed. Moreover, Degefe et al. (2024) assessed the upper Meki sub catchment in the Rift Valley sub-Basin and calculated a total annual soil loss of approximately 2,756,540 ton, resulting in an average estimated soil loss rate of 28.12 to 34.77 ton/hectare/year.

In Conclusion, the estimated soil loss rate of 32.84 ton/hectare/year in the Abaya Lake Sub Basin is consistent with the finding from multiple studies across Ethiopia.

To achieve a thorough understanding of soil erosion dynamics and enable meaningful comparisons across various partes of the watershed, the average soil loss in the study area was systematically categorized into five distinct severity classes of soil erosion. This classification framework was directly adapted from the research conducted by Kanito D. Bedadi B. Feyissa S. Kabo-Bah A. and Kaka S.L(2025). Which offers a standard method for assessing soil erosion risk.

In this context, the quantitative evaluation of soil erosion rate in the Abaya Lake Sub Basin was carefully calculated and organized into five ordinal classes. This classification not only helps identify the severity of soil erosion but also serves as an essential tool for land management and conservation planning. The findings from this analysis are presented in table 4.1, which outlines the various soil erosion classes based on the average annual soil erosion rates expressed in ton/hectare/year.

Table 4.1 Soil Erosion Risk Class

#	Soil Erosion Risk Class	Average Soil loss(t/ha/year)	Area	
			Ha	**%**
1	Low	0 – 5	0	0%
2	Moderate	5 - 15	9614.55	11%
3	High	15 - 30	28627.18	33%
4	Very High	30 - 50	34080.25	40%
5	Sever	>50	13724	16%
Total			**86,046**	**100%**

Source: Adopted from Kanito, D., Bedadi, B., Feyissa, S., Kabo-Bah, A. T., & Kaka, S. L. (2025).

The soil erosion severity classes presented in the above table revealed some concerning trend regarding soil erosion in the study area. A significant 40% of the sub basin falls into "Very high" risk category for soil erosion, in total a staggering 89% of the area is classified as experiencing "high" to "severe" erosion risk, while only 11% is considered to have a "moderate" soil erosion risk. This condition raises a serious alarm about potential soil degradation, which could negatively impact agricultural production and environmental health. Very alarmingly, there are no areas identified as having a "Low" risk, highlighting the pervasive issue of soil erosion in the Abaya Lake sub-Catchment.

This classification not only emphasize the urgent need of tackling soil erosion but also provide a foundation for targeted actions to mitigate its effects throughout the Sub-catchment. By understanding how soil loss severity is distributed, stakeholders can better allocate resources and develop management strategies that are specifically tailored to address the unique need of each risk categories.

4.2 Soil Erosion Dynamics in the Sub-Catchment

Soil erosion caused by water is a complex process that varies depending on time and location, influenced by several factors such as ground cover, soil texture, structure, porosity, permeability, and the lay of the land. Recent research has pointed out that, two critical processes i.e. detachment and dispersion, play a significant role in erosion, especially in soils that are cycles of wetting and drying can greatly affects both surface and internal erosion

(Panagos et al., 2022; Uber et al., 2024).

Human activities, particularly poor land management practices such as unsustainable farming and deforestation, worsen this erosion process by disrupting soil structure and diminishing plant cover (European commission JRC, 2023; Land Journal, 2025). For instance, large-scale simulation using change the global soil erosion model (GLOSEM) predicted that if the land use change continues unchecked, global soil erosion rate could surge by 30% to 66% by 2070, given current climate trend (Panagos et al., 2022).

Analysis of satellite data has shown notable shifts in land use, particularly, the expansion of agriculture onto steeper slopes, which heightens erosion risk even through the affected areas may be relatively small. These findings are consistent with trend in rainfall variability, climate change is altering precipitation pattern, which in turn intensifies erosion, especially in tropical and subtropical regions (Uber et al., 24; Panagos et al., 2022). For example, it is estimated that rainfall erosivity in humid tropical climate could increase by as much as 34% by 2070, leading to higher rate of soil detachment (Panagose et al., 2022).

The following section will delve into soil erosion rate and their changes over the past 30 years, incorporating advancement in remote sensing technology and high-resolution erosion modeling.

4.2.1 Estimated Soil Loss from the Sub-Catchment in 2003

Based on the study, it is observed that, there is a huge variation in the potential soil erosion rates, with some areas experiencing as low as 0.0 ton per hectare per year, while other faced erosion rate as high as 357.63 tons per hectare per year. The mean annual soil erosion rate across the entire watershed was calculated to be 24.79 tons per hectare per year. Which implies, over the course of the year, an estimated total of 2,133,079.84 tons of soil were lost, impacting the entire area. For a clearer understanding of these findings, see at figure 4.2 below, which illustrates the soil erosion potential map of 2003.

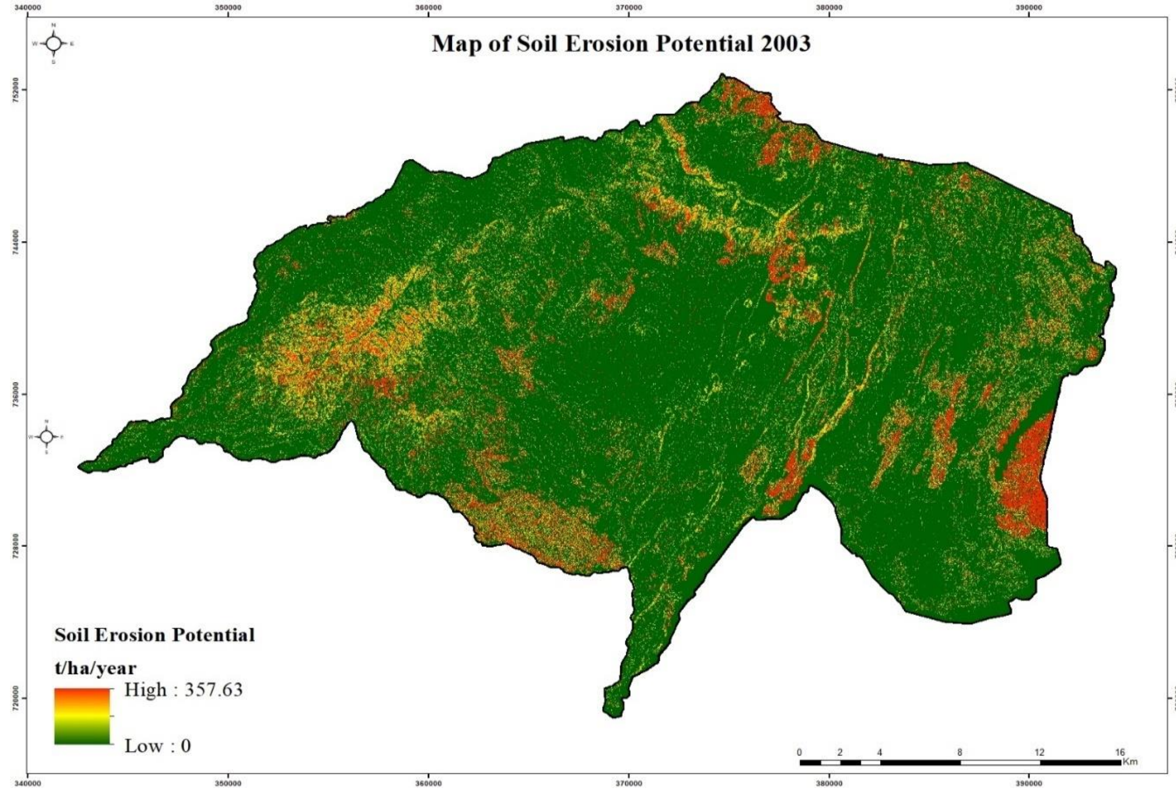

Figure 4.2 Soil Erosion Potential Map of 2003

4.2.2 Estimated Soil Loss from the Sub-Catchment in 2015

Based on the analysis the computed potential soil erosion for the year 2015 ranges from 0.0 to 451.878ton/ha/year and the average annual soil loss for the entire watershed was estimated to be 20.13 ton/ha/year. As compared with the average soil erosion rate of the year 2003, average soil erosion rate in 2015 has shown a decline by 0.38ton/ha/year. This is manly attributed to the land use land cover change in the study area coupled by the observed decline in rainfall erosivity factor between 2003/2015. Accordingly annual soil loss has decreased from 2,133,079.84tons to 1,732,105.57ton per year.

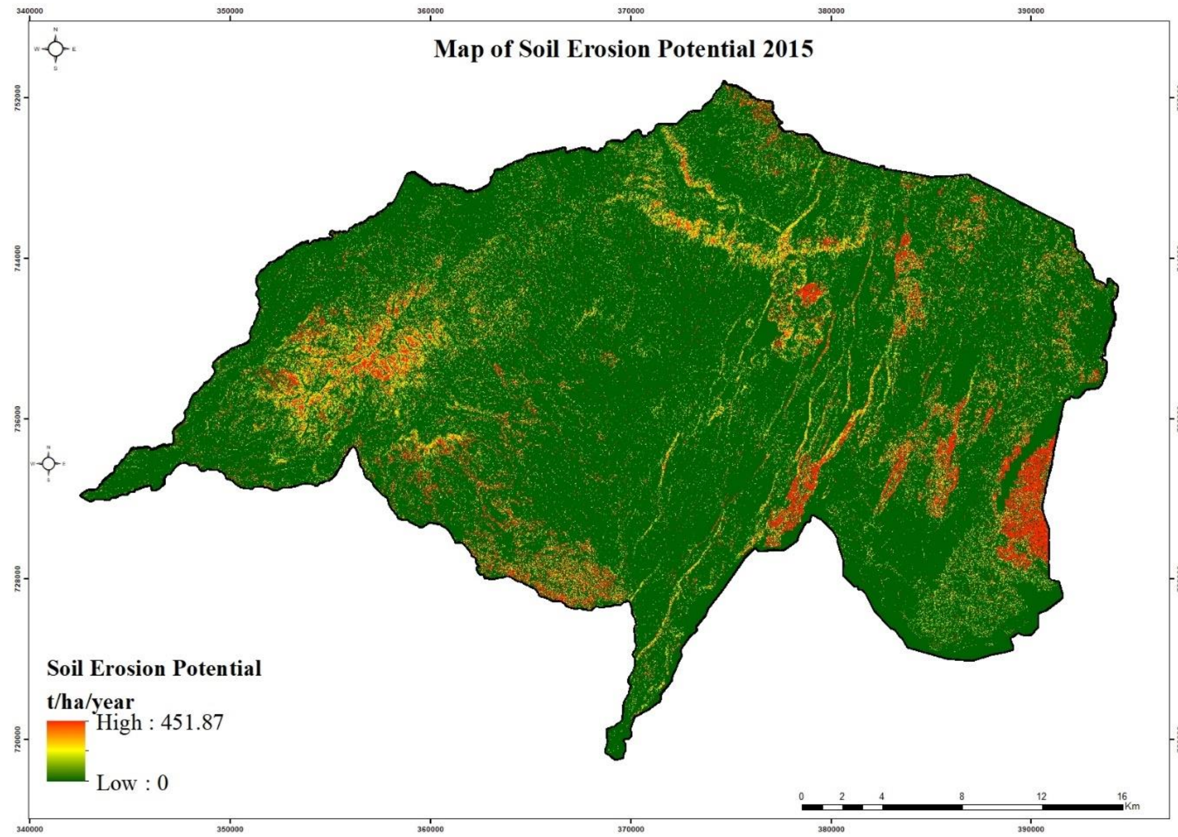

Figure 4.3 Soil Erosion Potential map of 2015

4.2.3 Estimated Soil Loss from the Sub-Catchment in 2025

The study estimates that by 2025, soil erosion rate in the Abaya Lake sub-Catchment varies significantly, ranging from 0.0 to 508.97 tons per hectare per year. Based on the findings, the study area is losing 32.84 tons of soil every year, leading to a total estimated loss of around 2,825,750 tons from the entire Sub-catchment.

While the results indicate an overall increase in soil erosion rates, looking much deeper in to the data, it is observed that soil erosion between 2003 to 2015 indicated a decline in soil erosion by 0.38tone per hectare per year. However, the soil loss rate rises up again between 2015 to 2025 showing an increase in soil erosion rate of 0.36 tons per hectare per year. We go back to 2003 and compare the soil loss rate with the 2025, it showed a general increasing trend in soil erosion rate of 1.27 tons per hectare per year. The slowdown in average soil erosion rate between 2003/2015 can be mainly attributed to the increase in homestead farming such as enset (false banana), as well as the introduction of multistory vegetation in the upper partes of the Sub-catchment. Figure 4.1 below shows the potential soil loss rates and their distribution within the Abaya Lake sub- Catchment.

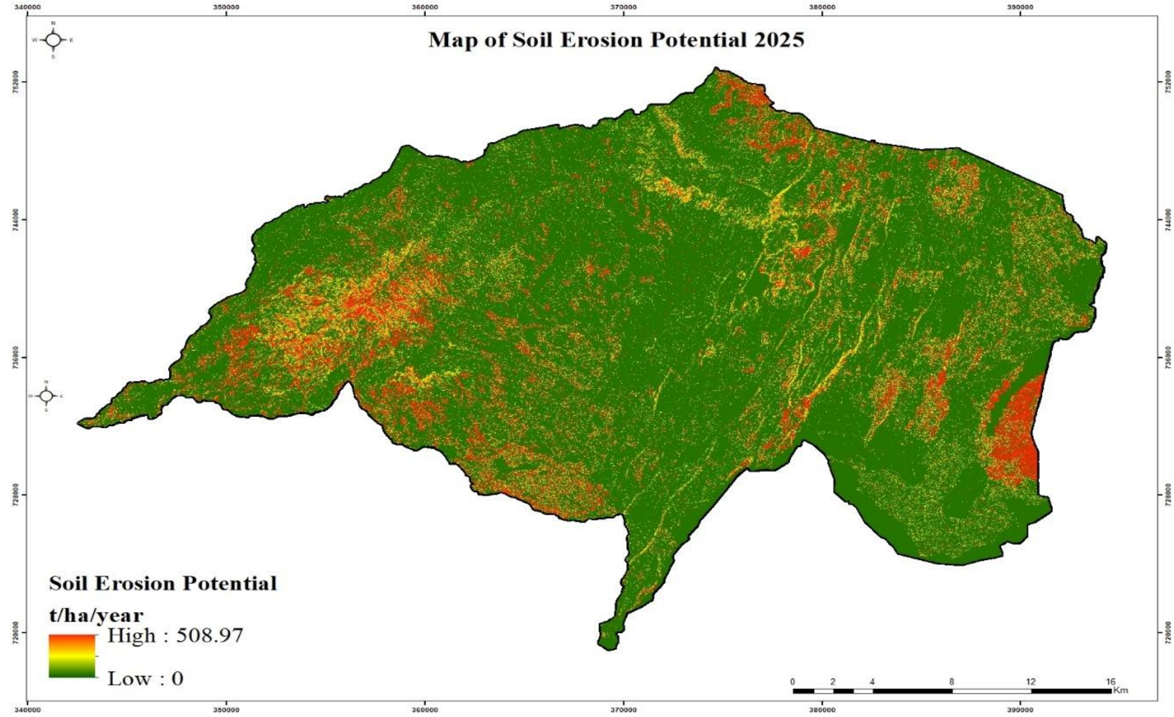

Figure 4.4 Soil Erosion Potential map of 2025

To better understand the spatial and temporal dynamics of soil erosion, soil erosion potential of the year 2003, 2015 and 2025 are classified in to 6 class and presented in figure 4.5 below.

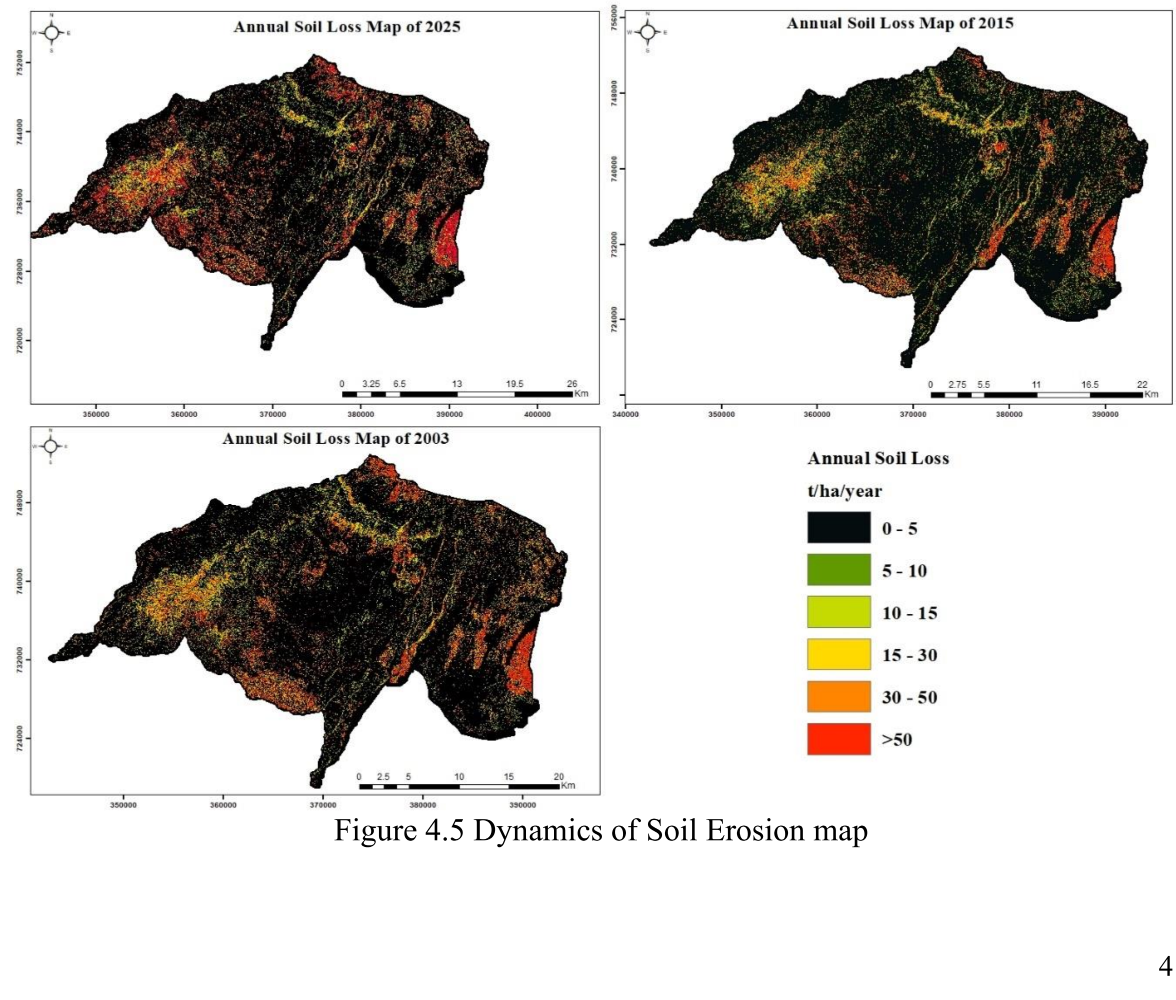

Figure 4.5 Dynamics of Soil Erosion map

4.3 Hotspots of Soil Erosion in in the Sub Basin

4.3.1 Identification of critical sub-watershed

Prioritization of sub-watersheds involves ranking the different sub-watersheds according to the order in which they ought to be taken up for conservation management, by taking into consideration the amount of soil loss occurring.

In this work, a total of 8 sub-watersheds were delineated based on drainage systems and the erosion risk map were reclassified based on prioritization. Figure 4.4 below shows the eight sub watersheds in the study area.

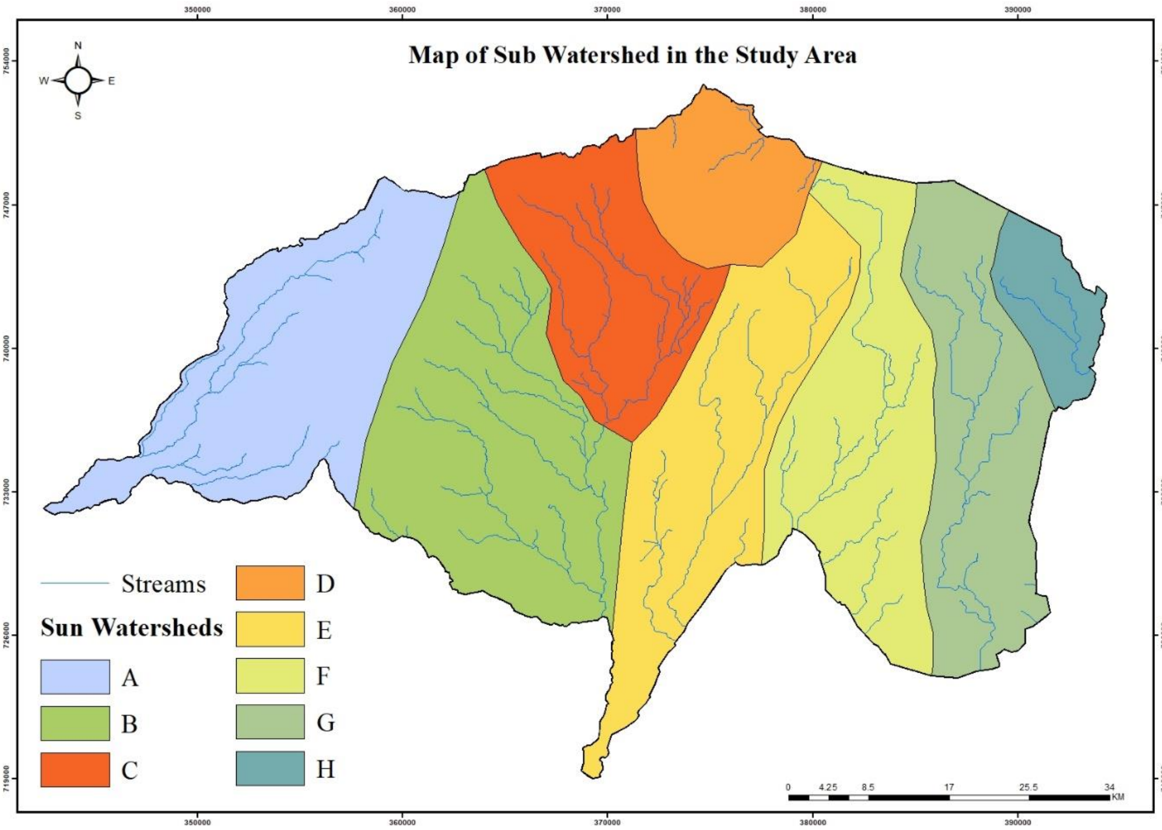

Figure 4.6 Map of Sub-Watersheds

Soil erosion risk maps and critical classes based on the distribution of soil loss for the Sub-catchment were computed using the average annual soil loss. According to Hurni (1983), the maximum tolerable soil loss rates for medium soils across various agro-ecological zones in Ethiopia range from 1 ton per hectare per year in the Berha agro-climatic zone to 16 tons per hectare per year in the Wet Weyna Dega agro-ecological zones (as cited by Israel Tessema et al. 2023).

For this study, the researcher adopted the soil erosion severity classification from Kanito, D., Bedadi, B., Feyissa, S., Kabo-Bah, A. T., Kaka, S. L. (2025), as discussed in the previous section. Accordingly, Table 4.2 below presents the average soil loss from the sub-watershed in the Abaya Lake sub-Catchment.

Table 4.2 Average Soil loss from the sub-watersheds

#	Watershed	Area (Ha)	Area (%)	Average Soil Loss (t/ha/yr)	Ranges of potential Soil lose(t/ha/yr)
1	A	13724	16%	58.50	0 – 508.79
2	B	17225.25	20%	43.38	0 – 293.08
3	C	9614.55	11%	14.25	0 – 93.49
4	D	5351	6%	35.60	0 – 101.13
5	E	13032	15%	15.17	0 – 84.65
6	F	12533	15%	19.40	0 – 272.50
7	G	11504	13%	37.80	0 – 63.91
8	H	3062.18	4%	20.84	0 – 69.04

As table 4.5 showed, sub watershed “C”, is classified under moderate soil erosion risk classes, while sub watershed while the rest falls from high to sever erosion risk class.

4.3.2 Prioritization for sub-watershed treatment

RUSLE was utilized for the identification and prioritization of the critical sub-watersheds on the basis of average annual soil loss. The predicted quantity of soil loss and its spatial distribution can provide a basis for comprehensive management and sustainable land use for the watershed. The areas with high and severe soil erosion warrant special priority for the implementation of control measures. Table 4.3 below shows erosion risk and priority class in the watershed.

Table 4.3 Erosion risk classes.

Soil loss(t/ha/y)	Severity classes	Priority classes	Sub Watersheds	Area(ha)	Area (%)
0 – 5	Low	VI	-	-	-
5-15	Moderate	IV	c	9,614.55	11%
15 - 30	High	III	H, F, E	28,627.2	33%
30 - 50	Very High	II	B, G, D	34,080.3	40%
>50	Sever	I	A	13,724	16%

The analysis of erosion risk classes within the sub-catchment, detailed in Table 4.3, highlights a troubling pattern of soil loss that calls for focused management efforts. The classification system identifies five levels of severity, and notably, no sub-watersheds fall into the low severity classless than 5 tons per hectare per year). Indicating that there are no areas experiencing minimum soil loss.

Sub-watershed “C” is categorized as having moderate severity)5 – 15t.ha/y) and covers 9,614.55hectars, representing 11% of the total watershed area. This suggests a need for ongoing monitoring and potential management strategies to address erosion in this region.

On the other hand, the high severity class (15 – 30 t/ha/y) includes sub-watershed “H”, “F”, and “E” which together make up 33% of the watershed area (28,627.2hectares). this significant proportion underscores the urgent need for targeted erosion control measures in these areas.

The very high severity class (30 – 50 t/ha/y) contains sub watersheds “B”, “G”, and “D” which accounts for substantial 40% of the watershed (34,080.3hectares). this indicates an immediate requirement for strong erosion control initiatives to protect these vulnerable regions.

Moreover, sub-watershed “A” falls into the severe category (more than 50 t/ha/y), covering an area of 13,724 hectares, or 16% of watershed. This classification highlights the critical need for immediate intervention in this area.

In terms of prioritization for treatment, sub-watershed “A” should be addressed first due to its sever erosion risk. Following that, attention should turn to sub-watershed “B”, “G”, and “D”, which are classified as very high severity class. Next in line are sub-watershed “H”, “F”, and “E”, which experience high level of soil loss. Finally, sub-watershed “C”, with its moderate risk, should be monitored to ensure long-term sustainability.

Overall, this analysis emphasizes the pressing need for effective management strategies to combat soil erosion throughout the Sub-catchment, particularly in the areas most severely impacted. Figure 4.7 below illustrate the soil erosion priority map for further insight.

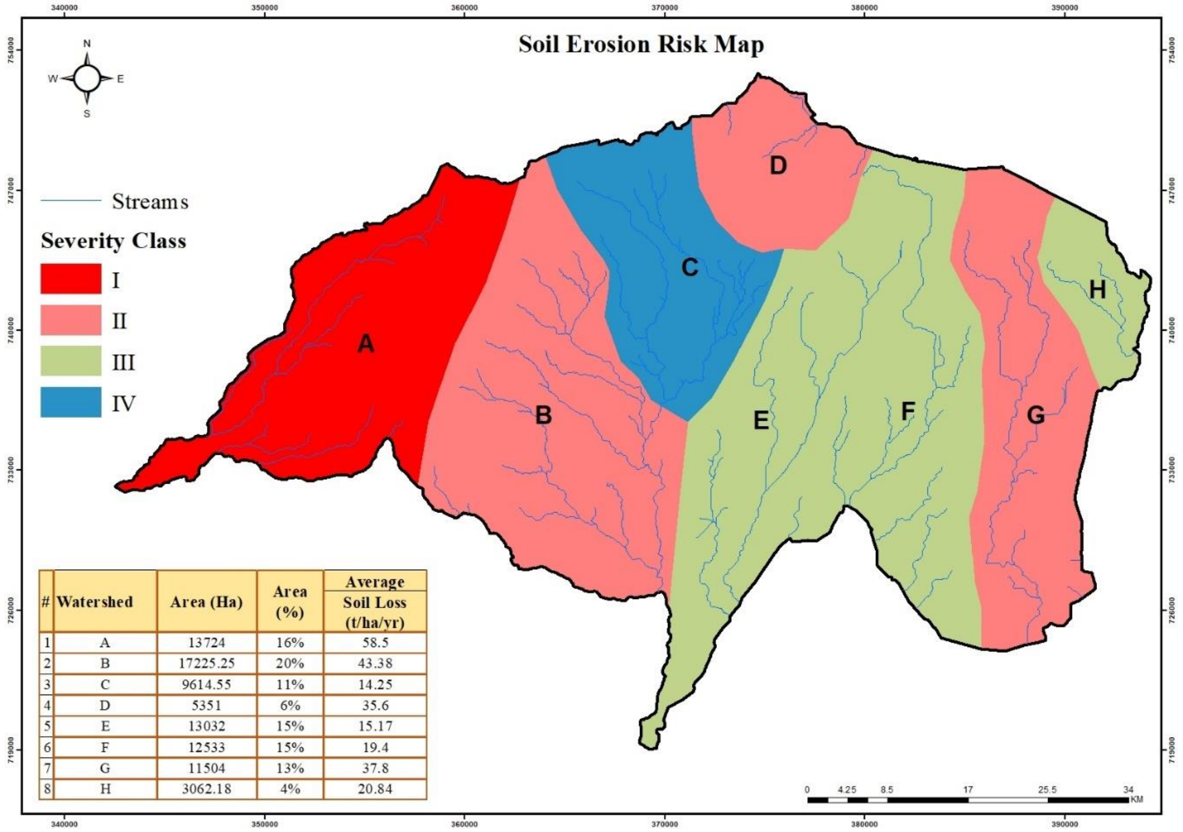

#	Watershed	Area (Ha)	Area (%)	Average Soil Loss (t/ha/yr)
1	A	13724	16%	58.5
2	B	17225.25	20%	43.38
3	C	9614.55	11%	14.25
4	D	5351	6%	35.6
5	E	13032	15%	15.17
6	F	12533	15%	19.4
7	G	11504	13%	37.8
8	H	3062.18	4%	20.84

Figure 4.7 Soil Erosion Risk Map

5. CONCLUSION AND RECOMMENDATIONS

5.1 Conclusion

This study attempts to find soil erosion extent, magnitude and dynamics from the year 2003 to 2025 due to change in precipitation and land cover changes based on estimating annual soil loss by applying RUSLE model integrated with Machin learning algorism in Abaya Lake Sub-Catchment. Based on the results and the further analysis, the following conclusions can be drawn.

Firstly, the RUSLE model integrated with the Fandom Forest classifier revealed that majority of the sub-catchment that accounts about 89% are potentially prone to soil erosion hazards. The current potential soil erosion rate in the sub catchment is estimated to be within the range of 0.0 to 508.97ton/ha/year. The average soil loss for the entire sub catchment was calculated to be 32.84ton/ha/year, leading to a total of 2.83tons soil loss from an area 86,046hecater.

Secondly the finding revealed that there was a significant increasing trend in mean annual soil erosion rate from 24.79ton/ha/year in 2003 to 32.84ton/ha/year in 2025, even though it has shown a decline in the amount of mean annual soil erosion rate by 0.38ton/ha/year between 2003 and 2015, and this is mainly due the observed a decline in rainfall erosivity.

The study also pointed out that variation in the distribution of mean annual soil erosion rate geographically. For instance, the highest average annual soil loss ranging from 0.0 to 508.97ton/ha/year is observed in the western part of the sub-catchment, while, the upper catchment and lower catchment exhibited 101.1ton/ha/year and 64.94ton/ha/year respectively. This spatial variability underscores the necessity for localized management strategies that account for the unique characteristics and vulnerabilities of different sub-watersheds within the sub-catchment.

The research also has tried to prioritize the sub-watersheds based on the average annual soil erosion rate. According to the study result, areas which are classified as sever erosion class covers an area of 13,72ha which is about 16% of the total sub-catchment while high and very high soil erosion risk class covers an area of 62,707.5 (73%) and moderate soil erosion risk class covers an area of 9,614.55ha (11%). For proper soil and water conservation treatment, the sub-watershed was then prioritized based on their severity class. The severe and very high soil erosion class was significant, which urges for appropriate conservation measures before the area is turned into level of irreversibility. Accordingly, top priority for soil conservation measures must be given to sub-watershed "A", in the first stage, sub-watersheds "B", "G", "D", can be considered in the second stage, sub-watershed "H, F, and

E” in the 3rd stage and finally sub-watershed “C” could undergo at last.

5.2 Recommendations

The results of soil erosion risk, severity, and land use/cover-type can assist decisionmakers in identification of priority areas in urgent need of conservation and land management plans. Majority of the study area (about 89%) is under high to severe soil erosion risk which merits urgent conservation measures. Based on the results of the study, it is recommended that immediate action should be taken to curb acceleration of the soil degradation.

Therefore, the researcher recommends the following soil and water conservation measures.

- In Gentle slope area (0 -5%): - to used level bunds and conservation tillage
- In Moderate slope area (5 -15%): - to implement contour farming combined with conservation tillage and physical structures like soil bunds.
- In Step Slope area (15 – 50%): - to use terrace combined with vegetation cove and stone-faced soil bunds
- In Very Steep Slope area (>50%): - to implement bench terraces, agroforestry, and permeant vegetation cover.

In any further soil and water conservation interventions (be it physical or biological conservation), the active involvement of the local community is important and the priority classes identified need to be taken to the forefront.

For sound soil and waters conservation plan, the researcher also recommend for further studies to be undertaken mainly that focuses on the main drivers of the soil erosion losses in the farming system (i.e., Socio-economic, agronomic and biophysical factors that trigger soil erosion) to establish the suitable soil and water conservation measures that should be implemented in Abaya Lake sub-Catchment, through the government and the participation of the farmers and villagers living across the watershed.

REFERENCES

Abebe, G., Tsunekawa, A., Haregeweyn, N., Adgo, E., Tsubo, M., Meshesha, D. T., Masunaga, T., & Yibeltal, M. (2020). Effects of land use and sustainable land management practices on runoff and soil loss in the Upper Blue Nile basin, Ethiopia. Science of the Total Environment, 728, 138776. https://doi.org/10.1016/j.scitotenv.2020.138776

Al-Abadi, A. M., & Al-Ali, A. A. (2018). Machine learning approaches for mapping soil erosion risk in the Diyala River basin, Iraq. Environmental Earth Sciences, 77, 353. https://doi.org/10.1007/s12665-018-7537-6

Anteneh, A., & Biru, T. (2021). Soil erosion assessment and mapping using RUSLE model and GIS in the Upper Blue Nile Basin, Ethiopia. Environmental Systems Research, 10, 18. https://doi.org/10.1186/s40068-021-00240-x

Arega, E., Deribew, K. T., Moisa, M. B., & Gemeda, D. O. (2024). Assessment of soil erosion and prioritization of conservation and restoration measures using RUSLE and Geospatial techniques: the case of upper Bilate watershed. *Geomatics, Natural Hazards and Risk*, *15*(1). https://doi.org/10.1080/19475705.2024.2336016

Atoma, H., Suryabhagavan, K.V. & Balakrishnan, M. Soil erosion assessment using RUSLE model and GIS in Huluka watershed, Central Ethiopia. *Sustain. Water Resour. Manag.* 6, 12 (2020). https://doi.org/10.1007/s40899-020-00365-z

Azedou, A., Kouassi, K. E., & Kouassi, B. (2023). Validation of LS factor estimation methods for soil erosion modeling in tropical mountainous landscapes. Catena, 217, 106582. https://doi.org/10.1016/j.catena.2022.106582

Azedou, S. E., Benabdelouahab, T., El Harti, A., El Mandour, A., & Boukdir, A. (2021). Random forest model for mapping water erosion susceptibility in the Oued El Abid watershed (High Atlas, Morocco). Geocarto International, 36(13), 1423–1440. https://doi.org/10.1080/10106049.2019.1678873

Bagegnehu Bekele, W., & Yenealem Gemi, T. (2021). Length-slope factors for the revised universal soil loss equation: Simplified method of estimation and application in Ethiopia. *ResearchGate*.

Bahadur J., Malla M., & Pant D. (2012). Assessment of Soil Erosion Risk Using Remote Sensing Techniques: A Case Study from Nepal. *Environmental Monitoring and Assessment*, 184(10), 6233-6246.

Belgiu, M., & Drăguţ, L. (2016). Random forest in remote sensing: A review of applications and future directions. *ISPRS Journal of Photogrammetry and Remote Sensing*, 114, 24–31. https://doi.org/10.1016/j.isprsjprs.2016.01.011

Benavidez, R., Jackson, B., Maxwell, D., & Norton, K. (2018). A review of the (Revised) Universal Soil Loss Equation ((R)USLE): with a view to increasing its global applicability and improving soil loss estimates. *Hydrology and Earth System Sciences*, 22(11), 6059–6086. https://doi.org/10.5194/hess-22-6059-20185

Bewket, W., & Teferi, E. (2009). Assessment of soil erosion hazard and prioritization for treatment at the watershed level: Case study in the Chemoga watershed, Blue Nile Basin, Ethiopia. Land Degradation & Development, 20(6), 609–622.

Borrelli P., Robinson D.A., & Panagos P. (2021). A New Model for Mapping Rainfall Erosivity in Europe. *Environmental Research Letters*, 12(6), 064019.

Borrelli, P., Robinson, D. A., Fleischer, L. R., Lugato, E., Ballabio, C., Alewell, C., ... & Panagos, P. (2017). An assessment of the global impact of 21st century land use change on soil erosion. Nature Communications, 8, 2013. https://doi.org/10.1038/s41467-017-02142-7

Borrelli, P., Robinson, D. A., Panagos, P., Lugato, E., Yang, J. E., Alewell, C., ... & Montanarella, L. (2021). An assessment of the global impact of 21st century land use change on soil erosion. Nature Communications, 12, 5237. https://doi.org/10.1038/s41467-021-25487-8

Breiman, L. (2001). Random forests. Machine Learning, 45(1), 5–32. https://doi.org/10.1023/A:1010933404324

CDM Project. (2009). *Project Design Document for the Humbo Ethiopia Assisted Natural Regeneration Project* (Version 02, UNFCCC Registration: 2728). United Nations Framework Convention on Climate Change (UNFCCC). https://s3.amazonaws.com/CCBA/Projects/Humbo_Ethiopia_Assisted_Natural_Regeneration_Project/PDD+of+Humbo+project.pdf

CIAT. (2024). *Nurturing Africa's Soil Health: Towards Zero Soil Loss and Runoff*. Alliance of Bioversity International and CIAT.

Congalton, R. G. (1991). A review of assessing the accuracy of classifications of remotely sensed data. Remote Sensing of Environment, 37(1), 35–46. https://doi.org/10.1016/0034-4257(91)90048-B

Congalton, R. G., & Green, K. (2009). Assessing the Accuracy of Remotely Sensed Data:

Principles and Practices (2nd ed.). CRC Press. https://doi.org/10.1201/9781420055139

Dai, L., Zhang, Y., & Li, S. (2022). Modeling the effects of slope length and steepness on soil erosion using RUSLE: A case study in the Loess Plateau, China. Catena, 208, 105695. https://doi.org/10.1016/j.catena.2021.105695

Dawit Bobe, G., et al. (2025). Soil erosion estimation and land degradation assessment in the Gununo watershed, southern Ethiopia. Environmental Systems Research, 14, 12. https://doi.org/10.1186/s40068-025-00200-5

Degefe, T., et al. (2024). Soil erosion assessment and sediment yield estimation in the Upper Meki sub-catchment, Rift Valley Basin, Ethiopia. Environmental Systems Research, 13, 45. https://doi.org/10.1186/s40068-024-00123-7

Degfie Teku, Tarekegn Derbib; (2025): Uncovering the drivers, impacts, and urgent solutions to soil erosion in the Ethiopian Highlands: a global perspective on local challenges. REVIEW article Front. Soil Processes Volume 12 - 2024 | https://doi.org/10.3389/fenvs.2024.1521611

Dereje, D., Mekuria, W., & Tadesse, T. (2006). Land degradation and soil conservation in Ethiopia: Historical perspective and current status. In Proceedings of the Workshop on Soil and Water Conservation (pp. 12–25). Ethiopian Agricultural Research Organization.

Dofee AA, Goshu F, (2024). Soil erosion impacts on crop productivity and its implications on food security in Kechabira district, Southern Ethiopia. AGBIR. 2024;40(6):1-11

Dumas, J., & Printemps, J. (2010). Soil erodibility assessment and its relation to soil properties in temperate regions. Catena, 81(1), 10–16. https://doi.org/10.1016/j.catena.2010.01.001

Efe, R., Ekinci, D., and Curebal, I.(2008). Erosion Analysis of Sahin Creek Watershed (NW of Turkey) using GIS Based on RUSLE (3d) Method. Journal of Applied Science, 8 (1), pp 49-58

Engel, B. A., et al. (2005). A GIS-based approach for estimating soil erosion potential using RUSLE: A case study from Indiana. *Journal of Soil and Water Conservation*, 60(6), 330-337.

European Commission Joint Research Centre (JRC). (2023). Soil erosion in Europe: Current status and future perspectives. European Soil Data Centre (ESDAC) Report.

Publications Office of the European Union. https://doi.org/10.2760/123456

FAO and IAEA. (2017). Soil erosion: The greatest challenge for sustainable soil management. A report from the Global Symposium on Soil Erosion, Rome, 15–17 May 2019. Food and Agriculture Organization of the United Nations and International Atomic Energy Agency, Rome, Italy. [Available online: https://www.fao.org/3/i9439en/I9439EN.pdf]

FAO, (1986). Soil Map of the World, Volume 1: Legend. FAO, Rome, Italy. Available at: http://www.fao.org/soils-portal/soil-survey/soil-maps-and-databases/soil-map-of-the-world/en/

FAO, (2015a). Status of the World's Soil Resources: Main Report. Food and Agricultural Organization of the United Nations (FAO). Accessed 8 November 2024.

FAO, 2017. Voluntary Guidelines for Sustainable Soil Management. Food and Agricultural Organization of the United Nations (FAO). Accessed May 2025.

FAO, 2020. Global Symposium on Soil Erosion. Food and Agricultural Organization of the United Nations (FAO). Accessed 8 November 2024.

FAO. (2015). Status of the World's Soil Resources (SWSR) – Main Report. Food and Agriculture Organization of the United Nations, Rome, Italy.

Fayas, M., et al. (2019). Assessment of soil erosion risk using RUSLE model in a semi-arid environment: A case study from Ethiopia. *Environmental Monitoring and Assessment*, 191(10), 641.

Fayera T.(2021). Assessment of the effectiveness biophysical soil and water conservation structures: a case study of kiramu woreda, east Wollega zone, Ethiopia, *Applied Research in Science and Technology*. (2021) 1, no. 2.

Feng, Q., Liu, J., & Gong, J. (2018). UAV remote sensing for urban vegetation mapping using random forest and texture analysis. Remote Sensing, 10(1), 146. https://doi.org/10.3390/rs10010146

Ferreira, J., & Panagopoulos, T. (2014). Seasonal cycles of the Cover Management Factor: Implications for soil erosion assessments. *Soil Use and Management*, 30(3), 345-356.

Feyera, S. (2021). Soil erosion and conservation in Ethiopia: A review. Environmental Systems Research, 10, 15. https://doi.org/10.1186/s40068-021-00232-0

Fikadu Israel, 2014. Assessing the impact of Afforestation/Reforestation on the Livelihoods of Local People: The Case of Humbo Woreda, Wolaita Zone. MA thesis, Addis

Abeba University, Ethiopia. Unpublished

Foody, G. M. (2002). Status of land cover classification accuracy assessment. Remote Sensing of Environment, 80(1), 185–201. https://doi.org/10.1016/S0034-4257(01)00295-4

Ganasri, B. P., & Ramesh, H. (2016). Assessment of soil erosion by RUSLE model using remote sensing and GIS: A case study of Nethravathi Basin. Geoscience Frontiers, 7(6), 953–961. https://doi.org/10.1016/j.gsf.2015.11.006

Gashaw, T., et al. (2020). Evaluating conservation practices for soil erosion control in Gilgel Abay watershed: Implications for sustainable land management in Ethiopia. *Sustainable Agriculture Research*, 9(3), 78-89.

Gashaw, T., Tulu, T., Argaw, M., & Worqlul, A. W. (2017). Modeling the impacts of land cover change on soil erosion using RUSLE and GIS: A case of the Andassa watershed in the Blue Nile Basin, Ethiopia. Environmental Systems Research, 6(1), 17. https://doi.org/10.1186/s40068-017-0084-7

Gitas, I. Z., Douros, K., Minakou, C., Silleos, N. G., & Karydas, C. G. (2009). Multi-temporal soil erosion risk assessment in N. Chalkidiki using a modified USLE raster model. Earth Surface Processes and Landforms, 34(3), 312–328. https://doi.org/10.1002/esp.1723

Goldblatt, R., You, W., Hanson, G., & Khandelwal, A. (2016). Detecting the boundaries of urban areas in india: A dataset for pixel-based image classification in google earth engine. Remote Sensing, 8(8), 634.

Goldblatt, R., You, W., Hanson, G., & Khandelwal, A. K. (2016). Detecting the boundaries of urban areas in India: A dataset for pixel-based image classification in Google Earth Engine. Remote Sensing, 8(8), 634. https://doi.org/10.3390/rs8080634

Golkarian, K. Khosravi, M. Panahi, J.J. Clague,(2023). Spatial variability of soil water erosion: Comparing empirical and intelligent techniques, Geoscience Frontiers

Gomez, C., White, J. C., & Wulder, M. A. (2020). Optical remotely sensed time series data for land cover classification: A review. ISPRS Journal of Photogrammetry and Remote Sensing, 158, 279–317. https://doi.org/10.1016/j.isprsjprs.2019.09.012

Gomiero, T., 2016. Soil degradation, land scarcity and food security: Reviewing a complex challenge. Sustainability, 8:281. Accessed 21 October 2020.

Haan, C. T., Barfield, B. J., & Hayes, J. C. (1994). Design Hydrology and Sedimentology for Small Catchments. Academic Press. ISBN: 9780124176513

Habtamu, T., Amare, T., Adgo, E., & Yitaferu, B. (2020). Soil erosion risk assessment using GIS and RUSLE model in the sub-humid Ethiopian Highlands. Environmental Systems Research, 9, 19. https://doi.org/10.1186/s40068-020-00185-z

Han, Y., et al. (2020). Impact of land-use and land-cover change on soil erosion using the RUSLE model: A case study from the Temeji watershed. *Journal of Water and Climate Change*, 12(7), 3404-3418.

Haregeweyn N., Tsunekawa A., Tsubo M., & Sano M. (2017). Soil Erosion Risk Assessment in Ethiopia: A Review on Methodologies Used Over Three Decades... *Land Degradation & Development*, DOI:10.1002/ldr.v28:5.

Humbo Woreda Disaster Risk Profile. (2020). Disaster Risk Profile Report, Humbo Woreda, Wolaita Zone, Southern Nations, Nationalities, and Peoples' Region (SNNPR), Ethiopia. Humbo Woreda Disaster Prevention and Preparedness Office.Hurni,

Hurni, H. (1983). Soil conservation in Ethiopia. In Soil Conservation and Management in the Tropics (pp. 123–135). Wiley.

Hurni, H. (1985). Erosion–productivity-conservation systems in Ethiopia. Soil Conservation and Productivity, 27–45. In: Soil Conservation and Productivity, Proceedings of the 4th International Conference on Soil Conservation, Maracay, Venezuela.

Hurni. (1988). Degradation and conservation of the resources in the Ethiopian highlands. Mountain Research and Development, 8(2/3), 123–130. https://doi.org/10.2307/3673238

IPBES, 2018. The assessment report on: Land Degradation and Restoration. Intergovernmental Science-Policy Platform on Biodiversity and Ecosystem Services (IPBES). Accessed 21 October 2020.

Iticha, B., & Takele, A. (2018). Estimation of soil loss rate using RUSLE model for Didessa sub-basin, Ethiopia. Environmental Systems Research, 7, 8. https://doi.org/10.1186/s40068-018-0117-x

Iticha, H., & Takele, T. (2018). RUSLE Model Based Annual Soil Loss Quantification for Soil Erosion Management. *SAGE Open*, 8(4), 11786221211046234.

Ji, C., Cao, Y., Li, X., Pei, X., Sun, B., Yang, X., & Zhou, W. (2024).A review of the satellite remote sensing techniques for assessment of runoff and sediment in soil erosion. Journal of Hydrology and Hydromechanics, 72(2), 252–267. https://doi.org/10.2478/johh-2024-0009

Kanito, D., Bedadi, B., Feyissa, S., Kabo-Bah, A. T., & Kaka, S. L. (2025). Spatial assessment of soil erosion for prioritizing efforts on SDG15.3 in Ethiopia. Frontiers in Remote Sensing, 6, Article 1550331. https://doi.org/10.3389/frsen.2025.1550331

Kidane, D., & Alemu, B. (2015). The effect of upstream land use practices on soil erosion and sedimentation in the Upper Blue Nile Basin, Ethiopia. Research Journal of Agriculture and Environmental Management, 4(2), 39–51.

Land Journal. (2025). The impact of land use change on soil erosion: A global perspective. Land, 14(1), 45. https://doi.org/10.3390/land14010045

Liaw & Wiener, (2002). Classification and Regression by Random Forest. Vol. 2/3, December 2002. ISSN 1609-3631.

Lillesand, T. M., Kiefer, R. W., & Chipman, J. W. (2008). Remote Sensing and Image Interpretation (6th ed.).

Lu, H., Nearing, M. A., & Stone, J. J. (2004). Rainfall-runoff-soil loss relationships for the WEPP model. Transactions of the ASAE, 47(5), 1603–1611. https://doi.org/10.13031/2013.18311

McCool, D. K., et al. (2021). Sensitivity of soil loss estimates to changes in slope length and steepness in RUSLE: Implications for land management. *Journal of Soil and Water Conservation*, 76(3), 244-256.

McHugh ML(2012). Interrater reliability: the kappa statistic. Biochem Med (Zagreb). 2012;22(3):276-82. PMID: 23092060; PMCID: PMC3900052.

Mengie A., Kassa H., & Abebe A. (2021). Assessment of Farmers' Practices on Soil Erosion Control in East Shewa Zone: Evidence from Field Experiments in Ethiopia... *Environmental Monitoring and Assessment*, DOI:10.1007/s10661-021-09293-8.

Meseret Melilo, Dawit Dalga (2019). Evaluation of Soil and Water Conservation Measures on Physico-Chemical Properties of two Watershed in Humbo Woreda, Southern Ethiopia. International Journal of Novel Research in Life Sciences Vol. 6, Issue 1, pp: (54-61).

Millward, A.A. and Mersey, J.E. (1999). Adapting the RUSLE to model soil erosion potential in a mountainous tropical watershed. Catena 38, 109-129.

Moges, A., Hailu, A., & Tesfaye, A. (2021). Land use/land cover change detection and its implication on soil erosion in the Upper Blue Nile Basin, Ethiopia. Environmental Monitoring and Assessment, 193, 350.

https://doi.org/10.1007/s10661-021-09024-7

Mohamad, M. A., Al-Sharif, A. A., & Al-Ghamdi, K. A. (2021). Application of machine learning algorithms for soil erosion prediction: A review. Environmental Monitoring and Assessment, 193, 438. https://doi.org/10.1007/s10661-021-09154-3

Mohebzadeh, H., Feizizadeh, B., Blaschke, T., & Jafari, S. (2022). Integrating Revised Universal Soil Loss Equation (RUSLE) and Random Forest (RF) model for soil erosion risk mapping in semi-arid regions. Environmental Earth Sciences, 81, 127. https://doi.org/10.1007/s12665-022-10317-5

Moore, I. D., & Burch, G. J. (1986). Physical basis of the length-slope factor in the Universal Soil Loss Equation. *Soil Science Society of America Journal*, 50(5), 1294-1299.

Morgan, R. P. C. (2005). Soil Erosion and Conservation (3rd ed.). Blackwell Publishing.

Morgan, R. P. C., Quinton, J. N., Smith, R. E., Govers, G., Poesen, J., Auerswald, K., ... & Styczen, M. E. (1998).

Mountrakis, G., Im, J., & Ogole, C. (2011). Support vector machines in remote sensing: A review. ISPRS Journal of Photogrammetry and Remote Sensing, 66(3), 247–259. https://doi.org/10.1016/j.isprsjprs.2010.11.001

Mustefa, M., et al. (2019). Spatial variability of soil erosion risk assessment in the Hanger River watershed, Ethiopia. Environmental Earth Sciences, 78, 567. https://doi.org/10.1007/s12665-019-8431-2

Nachtergaele, F., Petri, M., Biancalani, R., van Lynden, G., van Velthuizen, H., & Bloise, M. (2012). Land Degradation: Assessment in Drylands and Gaps and Needs. In: Lal, R. & Stewart, B.A. (Eds.), Advances in Soil Science: Soil Degradation in the United States: Extent, Severity, and Trends (pp. 209–234). CRC Press.[FAO Land and Water Discussion Paper 15]

Naipal, V., Reick, C., & Pongratz, J. (2014). From local to global scale soil erosion modelling – A sensitivity analysis of the RUSLE model. *Geophysical Research Abstracts*, 16, EGU2014-2131. https://epub.ub.uni-muenchen.de/71204/1/EGU2014-2131.pdf

Nearing, M. A., Foster, G. R., Lane, L. J., & Finkner, S. C. (1989). A process-based soil erosion model for USDA-Water Erosion Prediction Project technology. Transactions of the ASAE, 32(5), 1587–1593. https://doi.org/10.13031/2013.31039

Nearing, M. A., Foster, G. R., Lane, L. J., & Finkner, S. C. (1999). A process-based soil erosion model for USDA-Water Erosion Prediction Project technology. Transactions of the ASAE, 32(5), 1587–1593. https://doi.org/10.13031/2013.31039

Negash, M., et al. (2021). Soil erosion assessment using RUSLE integrated with GIS: A case study from Chogo Watershed in Ethiopia. *Environmental Monitoring and Assessment*, 193(6), 1-18.

Negese A, Fekadu E, Getnet H. (2021). Soil erosion assessment and sediment yield estimation in the Chereti watershed, Ethiopia. Environmental Monitoring and Assessment, 193, 345. https://doi.org/10.1007/s10661-021-09020-y

Nyssen, J., Poesen, J., Deckers, J., Haile, M., & Moeyersons, J. (2002). Impact of soil and water conservation measures on catchment hydrological response—a case study in the Northern Ethiopian Highlands. Soil and Tillage Research, 64(1-2), 1–13. https://doi.org/10.1016/S0167-1987(01)00231-7

Ouadja, M., et al. (2022). Assessing soil erosion through the implementation of the RUSLE model: A case study from North Africa. *Water Science and Technology*, 24(7), 2487-2498.

Ouadja, Y., Benabdelouahab, T., Azedou, S. E., El Harti, A., & Boukdir, A. (2022). Assessment of soil erosion risk using RUSLE integrated with GIS and remote sensing in the Oued El Abid watershed, High Atlas, Morocco. Geocarto International, 37(17), 4957–4975. https://doi.org/10.1080/10106049.2021.1883810

Panagos, P., Borrelli, P., Matthews, F., Liakos, L., Bezak, N., Diodato, N., & Ballabio, C. (2022). Global rainfall erosivity projections for 2050 and 2070. *Journal of Hydrology*, 610, Art.no.127865. https://doi.org/10.1016/j.jhydrol.2022.127865

Panagos, P., Borrelli, P., Meusburger, K., Alewell, C., Lugato, E., & Montanarella, L. (2015). Estimating the soil erosion cover-management factor at the European scale. Land Use Policy, 48, 38–50. https://doi.org/10.1016/j.landusepol.2015.05.021

Pereira, P., & Muñoz-Rojas, M. (2017). Soil degradation: A major cause, evidence of, and key variable used to assess and understand land degradation. In Impact of Agriculture on Soil Degradation II: A European Perspective (pp. 1–24). Springer, Cham. https://doi.org/10.1007/978-3-319-60669-9_1

Prasannakumar, V., Shiny, R., Geetha, N., & Vijith, H. (2012). Spatial prediction of soil erosion risk by remote sensing, GIS and RUSLE approach: A case study of Siruvani watershed in Attapady valley, Kerala, India. Environmental Earth Sciences, 64(4), 965–972. https://doi.org/10.1007/s12665-011-0913-3

Reda, A., and Hailu, A. H. (2017). Extensive utilization of inorganic fertilizers in ethiopian agriculture and its possible consequences on soil quality. *J. Integr. Agric. Sci.* 13 (4), 155–171. doi: 10.5829/idosi.wjas.2017.155.171

Renard, K. G., Foster, G. R., Weesies, G. A., McCool, D. K., & Yoder, D. C. (1997). Predicting Soil Erosion by Water: A Guide to Conservation Planning with the Revised Universal Soil Loss Equation (RUSLE). USDA Agriculture Handbook No. 703.

Renard, K.G., Foster, G.R., Weesies, G.A., McCool, D.K. & Yoder, D.C. (1997). Predicting Soil Erosion by Water: A Guide to Conservation Planning with the Revised Universal Soil Loss Equation (RUSLE). *Agriculture Handbook 703,* 1-251

Rojas, M., Ruiz, L. A., & Castro, M. (2021). Random Forest classification for land use/land cover mapping using Sentinel-2 imagery in tropical regions. Remote Sensing Applications: Society and Environment, 21, 100450. https://doi.org/10.1016/j.rsase.2021.100450

Romshoo SA, Yousuf A, Altaf S and Amin M (2021) Evaluation of Various DEMs for Quantifying Soil Erosion Under Changing Land Use and Land Cover in the Himalaya. Front. Earth Sci. 9:782128. doi: 10.3389/feart.2021.782128

Seifu Kebede and Fekadu Fufa (2023). Estimation of average annual soil loss rates and its prioritization at sub-watershed level using RUSLE: A case of Finca'aa, Oromiya, Western Ethiopia. Environmental Health Engineering and Management Journal 2023, 10(1), 41-50

Sharma, S., et al. (2023). Assessing the effectiveness of soil conservation practices using RUSLE: Evidence from field studies in India and Ethiopia. *Land Degradation & Development*, 34(2), 456-470.

Shi, Z. H., Cai, C. F., Ding, S. W., Wang, T. W., & Chow, T. L. (2002). Soil conservation planning at the small watershed level using RUSLE with GIS: A case study in the Three Gorge Area of China. Catena, 47(2), 117–129. https://doi.org/10.1016/S0341-8162(01)00180-9

Shi, Z., et al. (2002). Evaluation of soil erosion risk in a watershed using RUSLE and GIS:

A case study in China. *Journal of Soil and Water Conservation*, 57(4), 245-251.

Shibire.B., H. K, · J. K., H., S. S., and K. L., (2024): Impact of forest landscape restoration in combating soil erosion in the Lake Abaya catchment, Southern Ethiopia. Leibniz Centre for Agricultural Landscape Research (ZALF), Eberswalder Str. 84, 15374 Muncheberg, Germany

SOLitude (2025) - Lake Management: Different Types of Soil Erosion & How to Prevent Them: Accessed from https://www.solitudelakemanagement.com/different-types-of-soil-erosion-how-to-prevent-them/ date Accessed: May 2025

Tadele Labiso (2021). Land suitability analysis for surface irrigation in Humbo woreda, wolaita zone, Southern Ethiopia. EQA - International Journal of Environmental Quality ISSN 2281-4485 - Vol. 44 (2021): 32-43

Tadesse, T., Abegaz, A., & Desta, H. (2021). Assessment of soil erodibility factor (K) for soil erosion modeling in the Ethiopian highlands. Environmental Systems Research, 10, 25. https://doi.org/10.1186/s40068-021-00245-5

Tatjana D. Golubović (2022): Prevention and Management of Soil Erosion and Torrential Floods: page 20: © 1988-2025, IGI Global Scientific Publishing: DOI: 10.4018/978-1-7998-8459-0.ch006

Tesfaye, B., & Tibebe, D. (2018). Soil loss estimation using RUSLE model in Megech watershed, Ethiopia. International Soil and Water Conservation Research, 6(4), 329–338. https://doi.org/10.1016/j.iswcr.2018.06.002

Tessema, I., Simane, B., & Kassa, K. (2023). Soil erosion estimation and risk assessment at watershed level: A case study of Neshe Dam Watershed in Blue Nile River basin, Ethiopia. International Journal of Environmental Science and Technology. Advance online publication. https://doi.org/10.1080/15715124.2023.2209324

The European Soil Erosion Model (EUROSEM): A dynamic approach for predicting sediment transport from fields and small catchments. Earth Surface Processes and Landforms, 23(6), 527–544. https://doi.org/10.1002/(SICI)1096-9837(199806)23:6<527::AID-ESP899>3.0.CO;2-4

Tiruneh, A., & Ayalew, D. (2015). Soil erosion risk assessment using RUSLE and GIS in the Upper Blue Nile Basin, Ethiopia. International Journal of Environmental Science and Technology, 12, 3537–3548. https://doi.org/10.1007/s13762-015-0784-3

Titmarsh G 2018, 'Determination of RUSLE soil erodibility (K) factors for Mining Lease (ML) 70481, Kestrel mine', report prepared for Kestrel Coal Resources Pty Ltd.

Uber, M., Haller, M., Brendel, C., Hillebrand, G., & Hoffmann, T. (2024). Past, present and future rainfall erosivity in central Europe based on convection-permitting climate simulations. *Hydrology and Earth System Sciences*, 28, 87–102. https://doi.org/10.5194/hess-28-87-2024

UCN, (2015). Land Degradation and Restoration: Global Environmental Outlook (GEO-5) for Business: Impacts of a Changing Environment on the Corporate Sector. IUCN, Gland, Switzerland.

UN (2003): "Resettlement 2003, Disaster Prevention and Preparedness Agency (DPPA) (accessed 16 May 2025)

UN (2003): Resettlement as a Response to Food Insecurity: UN-EUE Report May/June 2003 (accessed 16 May 2025)

United Nations (UN), (2015). Sustainable development. Department of Economic and Social Affairs. Accessed 16 May. 2025.

Wagari, A., & Tamiru, S. (2021). Estimation of soil erodibility factor (K) using soil color and texture for soil erosion assessment in Ethiopia. Soil and Water Research, 16(3), 150–160. https://doi.org/10.17221/45/2020-SWR

Wang, B., Xu, Y., Liu, D., & Zhang, S. (2016). Comparison of soil erosion modeling using RUSLE and RF models in the Loess Plateau of China. Catena, 147, 113–121. https://doi.org/10.1016/j.catena.2016.07.002

Wassie, S. B. (2020). Natural resource degradation tendencies in Ethiopia: a review. *Environ. Syst. Res.* 9 (1), 33–29. doi:10.1186/s40068-020-00194-1

Wischmeier, W. H., & Smith, D. D. (1978). Predicting rainfall erosion losses: A guide to conservation planning. U.S. Department of Agriculture, Agriculture Handbook No. 537.

World Bank, (2021). Ethiopia Climate Change Knowledge Portal: Country Profile. World Bank Group. Available at: https://climateknowledgeportal.worldbank.org/sites/default/files/2021-05/15463A-WB_Ethiopia%20Country%20Profile-WEB.pdf

Yin, S., Zhang, X., Liu, B., & Wang, Y. (2023). Advances in rainfall erosivity estimation and its application in soil erosion modeling: A review. Journal of Hydrology, 615, 128809. https://doi.org/10.1016/j.jhydrol.2023.128809

Yonas, M., Tadesse, T., & Abebe, A. (2021). Land cover classification of Ethiopian highlands using high-resolution satellite imagery and Random Forest algorithm. Remote Sensing Applications: Society and Environment, 22, 100482. https://doi.org/10.1016/j.rsase.2021.100482

Zhang, X., Liu, L., Wang, R., Wang, J., & Yu, D. (2018). A random forest model integrated with spatial analysis for land use/land cover classification in the urban fringe of the Yangtze River Delta, China. Remote Sensing, 10(4), 563. https://doi.org/10.3390/rs10040563

APPENDICES

Appendix 1: Climatic data

1. Bele Station

Year	Jan	Feb	Mar	Apr	May	Jun	Jul	Aug	Sep	Oct	Nov	Dec
2007												0
2008	8.4			112.7	52.9	52.5			30.1	134.4	27	0
2009	16.2	0	19.8	94.1	24.4	75.5	88.4		19.7	72.9	26.2	49.3
2010	0	90.6	96.8	192.7	106.3	17.8	213	220.3	75.1	26.1		
2011		4.4	12.1	42	96.6	112.9	247	501.1	327.5	0	0	0
2012	0			113.4	33.1	62.4	152.9	212.7	141	0	51.2	
2013					111.3	82.7	134.1					
2014	0	0	105.3	81.8	132.5	29.8	135.5	223.2	162.8	173.2	25.2	0
2015	0	0	5.5	107.1	151	168.6	51.8	148.9	66	53.9	56.7	0
2016	20.4	3	27.3	190	78.4	103.9	84.6	127.8	134.6	51.8	56.2	25.2
2017	0	3	50.7	75.7	135.4	4.9	54.8	180.1	125.4	76.6	59.8	
2018					97			133.9	64	86.9		
2020				135.6	141.5	139.2	230.3		70	24.7	30.5	21.2
2021			3.8	118.2	174.2		155.9	325.2	122.5	145.1		
2022	0	0	10.3		22.5	41.9	266	240.1	173.7			
2023	15	14.6	97.4	169.7	44.6				173	136.9	116.5	0
2024	0	3.2	70.3	89.1	42.5				86	138.4		

Source: ENMA (2025)

2. Dinke Station

Year	Jan	Feb	Mar	Apr	May	Jun	Jul	Aug	Sep	Oct	Nov	Dec
1988						94.7	200.2	143.4	169.4		0	2.3
1989		153.2	78.7	304.8	68.4	77.4		180.5	385.8	53	46	10
1990	0	194	187.8	130.2		79.2	142.7	154.3	169.4	12.6	96.1	61.7
1991	89.3	154.6	263.8	174.6	329.1	153.2	44	10	23.9		11.6	25.9
1992	0	15.6	80.6	154.2	141.5	210.6	138.7	123.1	188.2	140.8	17.4	57.6
1993	93.8	88.3	64.7	257	292.1	104.8	90.2	102	130	55.7	5	0
1994	0	61.1	131	191.6	190.1	112.9	148	207.4	99.8	74	114.1	0
1995	0.2	39.8	71.1	184.6	110.4	104	120.6	142	158.5	83.7	28.5	14
1996	17.3	25.1	176.6	240.1	213	181.5	127	117.2	130.1	15.4	62.8	0
1997	13.1	0	35.7	230.7	75	102	137.7	187.6	99.8	324.5	295.3	53.2
1998		43.1	71.7	137.9	199.7	115.5	75.4		67.5	215.5	28.6	5.8
1999	10	0.5	145.7	84.9	70.3	106.8	184.5	104.6	91.4	260.3	39.6	4
2000	0.5	0	8.3	83.6	222.5	90.6	121	118.3	128.8	142.9	72.6	23
2001	6.8	20.9	192.6	186.3	235.6	211.8	97.9	193.8	226.4	265.5	3.9	15.4
2002	31	19	134.9	65.4	133.1	64.7	107.4	116.8	161.7	119.7	6.5	122.7
2003	38	14.3	77.2	349.6	99.6	211	194	331.2	120.8	67.8	34.9	19.7
2004	130.5	39.3	13	293.8	77.2	85.2	140.7	121.6	134.2	62.8	121.1	44
2005	22.2	10.3	132.5	223.6	413.3	113.5	145.5	107.4	134.4	118.3	29.7	0

2006	3.2	93.7	151.3	207.3	142.9	115.8	148.5	134.2	172.7	270.9	70.7	115.5
2007	46	61.1	61.2	156.7	142.8	190.2	125	171.5	247.5	99	31	0
2008	4.3	23.5	40.2	164.6	166.4	117.4	191.8	186.3	164.9	126.6	60.2	0
2009	14.8	5	65.1	159.7	79.2	108.2	41	149.1	98.7	165.6	27.3	89
2010	27.2	77.7	195.4	240.2	333.7	119.7	88.4	81.6	121.4	140	14.8	31.6
2011	5.3	14.4	63	95.4	209.2	100.6	97.4	147	165.8	54.2	158.7	0
2012	0	5.6	27.6		117.8	62.6	109.5	95.6	174.1	14.8	66.2	16.4
2013	41.2	31	15.1	166.7	179	104.4	121.9	161.8	149.4	135.1	65.4	0
2014	0.1	82.3	91.8	149.4	195.2	188.2	74.2	164.2	170.1	163.1	144	0
2015	0	16.1	111.4	133.9	195.2	186.9	74.2	174.8	183	204.2	144.5	0
2016	26.7	0	106.8			288.9	72.6	58.5	128.1			0
2017	2.5	19.9	15.5	37.6	134.3	39.3	206.4	215.9	280.4	281.1	73.6	0
2018	2.4						31.8		84	118.5	159	
2019	0	0.9				159.8	170.5				122.9	81.9
2020	129.9	84.5	150.7	260.1	197.7			221.3	114.6	93.5	79.1	
2021	12.5	57.7	2	235.2	148.1	31.2	83.8		111			
2022	10.8	24.9	42.1	127.9	61.2	21.9	58.1	28.6	120	91		

Source: ENMA (2025)

3. Mayokota Station

Year	Jan	Feb	Mar	Apr	May	Jun	Jul	Aug	Sep	Oct	Nov	Dec
1990					106.3	121.6	137.1	171.5	77.1	9.2	17.2	
1991	39	82.9	157.4	187.7	260.3	168.2		208.2	59.3	18.2	12.6	21.8
1992	5.8			42.2	136	265.6	454.3	478.6	148.3	57.6	120.8	39.6
1993	91.1	122.6	18.9	234.1	387.9	135.2	107.1	173.6	58.9	52.2	3.2	3.8
1994	2.2	10	112.2	140.2	187.2	122.1	290.5	205.2	61.8	11.8	32.8	7.2
1995	0	117.1	83.2	232.9	91	188.4	146.4	127	201.2	107.5	21.9	38.7
1996	23.2	110	108.4	283	461.6	511.4	455.4	228.4	205.2	41.8	35	0
1997	4.6	0	41.7	237.1	505.4	161.5	103.5	48.6	84.7	290.5	366.6	25.3
1998	51.5	88.9	28.9	176.1	181.8	206.5	295.6	316.7	34.3	367.6	12.2	7.4
1999	34.2	7.4	87.5	97.7	169.7	58.9	173.7		155.5	252.5	26.7	34.6
2000	0	0	27.1	104.3	232.5	159.8	203.6	207	192.8	416.1	196	33.4
2001	18.8	66.8	182.3	162.9	370.4	177.1	277.6	416.7	64.1	96.8	46.5	19.8
2002	62.4	20.8	203.9	105.1	109.5	84.3	83.4	76.7	46.6	42.5	21.4	191.1
2003	109.8	40.3	105.6	275.3	155.4		136.1	233.9	76.7	66.9	66.7	70.8
2004	73.3	6.3	24.6	227.3	116.3	25.5	60.1	142.7	153.4	38	21.9	38.7
2005	51.7	19.4	52.8	398.5	548	73.6	424.5	157	209.8	137.6	112	12.2
2006	4.2	31.6	157.9	242.1	69.9	32.8	134.4	339	57	176	38.3	93.5
2007	58.6	42.2	90.7	152	116.1	195.7	335.4	392.2	195.2	3.4	0	0
2008	4.2	17.7	0	153.9	47.2	134.1	187.6	223	310.8	291.7	192.5	0
2009	11.8	22	60.5	79.3	28.1	98.6	134.7	110	81.1	181.9	107	216.6
2010	16.7	122.1	247.8	457	504.9	264.8	232.2	208.5	135	48.5	10	2.5
2011	0	9.6	3	110.4	225.7	121.8	229	317.9	252.3	7.7	35.4	9.2

2012	0	0	0	192.6	253.6	86.4	417.2	460.1	354	5.1	61.4	10.6
2013	55.3	31.4	212.9	502.7	249.6				129.7	148.3	53	0
2014	0.9	66	64.1	121	168.8	96.2	85.6	135.4		132.1	89.5	0.3
2015	10.3	9.1	43.5	133.7	58.6	96.3	93.9	75.7	47.6	80.7	231.8	40
2016	53.5		87.7	307.6	253	136.1	111.9	0	0	105.1	4.5	4.3
2017	4.3	55.2	21.8		183	51.7	186.9	174.3	236.3	205.7	63.4	
2018		63.5	54.5	282.2	427.3	227.6				39.7	139.3	0
2019	0		13.4	125.1	114.4	220	188.8	224.6	85.5	187		22.4
2020	74.6	149.8	86.1	226.1	289.6	121.7		271.1	148.2	126	35.2	20.2
2021	0		0.8			60.1	332.9		99			
2022	25.8	37.4	47.1	95.4	67.6	62.7	147.4			128	35.8	42.8

Source: ENMA (2025)

4. Wajifo Station

Year	Jan	Feb	Mar	Apr	May	Jun	Jul	Aug	Sep	Oct	Nov	Dec
1980			34.4					48.1				
1981			273.5	188.4	136.2	86	183.3	37.7	62.8	29.4	28.1	0
1982	14.3	27.3	64.6	50.9	259.9	30.4	89.1	49.8	31.1	76.8	210.9	79.2
1983	5.1	11.5	12.9	101.8	128.5	31.5	119.8	202	23.9	100.8		27.4
1984	0	40	21	8.2	63.8	57.5	26.4	37.3	59.3		31	20.5
1985	21.2	2.4			21.2		77.1	36	28.5			
1986		18.8	54	90.5	345.1			238.1	15.9			
1997	0.2		2.4	311.1	14.8	127.3	153.7	47.1	20.8	105.8	84.7	10.9
1998	11.8	25.4										
1999			54.6	58.5	53	84	91.1	93.8	64.8		36	8
2000		0	2.1	70	107.4	113.8	112.5	117.3	31	68.7	71.3	
2001	21.6	10.3	63.1	158	159.8	225.6	236.7	206.2	62.4	164.7	48.3	16.7
2002	14.1	0	70	187.7	87.8	49.5	27.7	151.1	51.6	25.9	4.1	97.9
2003	46.7	4.2	5	100.7	139.2	87.5	160.4	405	52.7	9.8	14.3	91.4
2004	67	14.2	0	264.3	51.2	28.3	111.5	189.8	59.3	31.7	91.2	109.2
2005	21.2	22.4	164.6	125.1	384.4	77.9	201	65.6	312.7	60.9	21.4	0
2006	21	35.4	174	343.3	209.2	137.8	147.9	351	32.7	296.1	255.9	137.8
2007	46	27.9	129.6	171.6	255.6	223.4	181.1	304.7	146.1	17.8	16.7	0
2008	2.8	0	22.9	107.9	112.6	26.8	206.6	146	164.6	166.6	169	0
2009	43.9	2	14.3	90.7	123.2	30	56.8	64.9	21.2	173.7	18.5	75.3
2010	9.6	56.8	328.5	228	218.1	135.2	59.8	266.4	62.3	40.6	0	20
2011	0	6.7	8.8	42.5	186	279.1	240.4	215.7	94	116.2	30.2	2.5
2012	0		2	135.4	41.6	94.4						
2013											44.5	
2014		21				82				162	24.5	0
2015	0	0	76	30	130	118	37.5	40	0.2	12.5	127	36
2016	10	13	35	201	108	35	4	44	16		18	
2017		0	31	40	208.5	0	148	148	156	154	16	0

2018	0	29	52	232.1	198		14.5	163		63.5	94.5	
2019	0		0	99.5	132.5	315	93				127	72.6
2020	58	71.7	149.7	118.5	291	152.5	128.5			123.5		
2021	0	24.5	0	120.5	214.5	25			142.5			
2022		0	0	0	0	59	34		154	50		

Source: ENMA (2025)

5. Bedesa Station

Year	Jan	Feb	Mar	Apr	May	Jun	Jul	Aug	Sep	Oct	Nov	Dec
1980			14.1		27			231.7	151.9	60.2	84.6	0
1981	0	39	176.7	57.3	134.8	21.6	41.9	269	366.8	67.2	15.1	0
1982	2.1	11.7		159.6	102.9	82.2	81.9	110.2	96.4	0	65.5	0
1983	0	20.8		137.7	308.3		159.4	272.1	240.9	81.8	0	0
1984	0	0	38.8	19.9	150.8	66.8	120.1	136.6	145.9	13.3	7.5	11
1985	0	0	64.5	167.5	128.8	59	181.5		89.1	19.7	18.1	15.1
1986	0	54.7	31.8	128.3	232.6	230.7	113.9	114.9	89.4	45.1	0	1.6
1987	0	16.8	143.8	89.4	253.5	22.8		31.1	127.6	47.7	0	0
1988	5.2	25	0	245.3	0	181		201.6				
1989					23.2		80.6	152.1	184.7		16.9	66.1
1990	3.2	102.9	50.2	219.3	56.5	40.9	121.9	170.8	194.4		4.8	
1991	1.5	50.6	201.9									
1994							226.9	155.1	190.1	58.4	16.2	0
1995	0	56.9	102.6	257.3	77.5	55.4	224.2	126.2	129.1	34.2	0	8.9
1996	37.2	9.4	117.2	191.4	178.7	133.6	154.9	164	164.6	32.7	40.2	1.3
1997		0	149	105.3	87	195.7	173.1	95.2	70.4	307	133.2	5.8
1998	49.1	30.9	30.2	102.8	165.4	123.3	161.9	92.6	138.5	155.8	18.6	0
1999	9	0.6	135.4	75.4	76.3	92.3	215.2	211	132.3	301.9	26.3	0.5
2000	0	0	16	127.8	142.2	63.1	136.3	167.1	214.3	146.7	97.3	14.2
2001	0		58.8	106.4	149	109.3	165.8	153.4	181.7	41.9	7.4	17.2
2002	16.5	0	69.6	48.2	106	56.3	108.1	150.8	94.9	50.5	0	72.2
2003	1.5	0	55.2	117.2	65.9	136.2	211.8	149.1	106.3	3.2	18.3	10.8
2004		0	55	338	33.7	77.2	153.3	117.3	258.1	135.2	18.8	31.2
2005	9.3	2.1	99.3	191.1	215.2	66.3	178.7	138.2	152	50	58	0
2006	2.6	8.9	71.4	187.9	101.4	73.8	127.1	215.1	212.4	92.5	1	75.4
2007	0	11.9	55.4	126.9	105.1	98.4	166	190.9	309	53.8	5.3	0
2008	0	0	0	165.1	172.2	41.3		222	140.5	50.7	93.4	0
2009	20.5	0.7	54	126.7	45.4	67.9	134.7	148.1		84.5		22.6
2010	2.2	87.7	202.5	280	335.9	48.2	278.5	162.3	254.7			0
2011	0	0	16.4	19	144.8	244.6	99.5	223.8	280.3	37.9	25.8	0
2012	0.2	0	18	123.3	18.7	185.6	178.6	195.4	322.6	9.8	1.2	15.7
2013	17.2	0	144.8	183.4	77.4	52.8	205.6	139.9	276.3	105.6	63.6	0
2014	0	0	152.8	119.4	99.3	32.6	105.6		166.6	201.8	16	0
2015	0.3	0	22.3	24.6	149.5	140.3	53	109.2	113.2	54.1	37	24

2016	68.6	0	14.6	225.4	147.7	58.5	147.3	41.5	103.7		38	
2017		0	49.4	77.2		51.6	68.5			5.1	3.2	0
2018	0	22.7	50.1	196.7	144.1	121.4	57.3	109.1	54.3	79.4	22.9	
2019	1.1	20.4	0.5	73.6	115.6	110.7	140.6	171.4	241.3	115.6	67.6	36.7
2020			89.8	189.2	240.1	92.1			135.7	68.4	31.7	10.9
2021	0	0		171.5	205.4	94.3				95		
2022	0.4				9.5	135.8		102.7	108.3	64.6	32.4	
2023	11.6	7.6	153.3	217.5	227	142.3	68.4			125.4		
2024											44.5	

Source: ENMA (2025)

6. Gessuba Station

Year	Jan	Feb	Mar	Apr	May	Jun	Jul	Aug	Sep	Oct	Nov	Dec
1995					54.7	99	226.7	189.4	133.6	85.4	15.6	23.7
1996	114.5	18.8	185.2	231.1	151.2	133.4	155.5	89.4	135.5	37.1	45.5	0.6
1997	11.7	0	17.1	238.1	159.9	121.7	81.7	35.9	59.6	320	204.5	48.7
1998	56.7	36.2	88.2	171.8	145.3	119	146.8	148.5	69.7	204.9	6.6	0.7
1999	12.4	1.3	109.8	113.6	128.9	88	155.6	164	94.4	185.4	24.7	5.3
2000	0	0	44.1	143.4	175.9	94.9	154.9	155.5	154.5	178.8	45.3	32
2001	9.7	3.6	77.9	138.6	191.5	134.5	76.2		42.7	15.7	2.8	6.7
2002	120.5	8.3	94.6	52.2	31	41.9	28.1	51.1	53.6	84.6	0	103.8
2003	63.6	9.4	22.9	434.8	72.5	173.5	190.1	125.6	36.4	24.5	73.4	40.5
2004	65.4	15.6	31.6	213.4	62.4	78.8	158.1	48.2	99.4	59.3	4.2	13.2
2005	14.3	6.3	108.1	135.3	83.6	118.7	45.4	58.6	135.7	117.2	20.9	2.8
2006	15.1	45.4	125.2	156.5	108.9	122.3	121.1	279.7	57.5	115.1	27.3	98.7
2007	34.2	6.9	107.3	68.7	176.2	89.6	87.5	196	169.6	21.9	4.4	0
2008	19.4	7.3	24.4	150.6	137.1	155.6	217.8	65.7	114.7	231.3	17.5	16.9
2009	34.2	6.9	107.3	68.7	176.2		87.5	59.6	103.3	128	54.4	92.3
2010	10.1	65.9	151.7	190.8	219.8	59.9	92.3	69.1	86.1	30.3	0.4	0.2
2011	8.9	4.4	32.4	72.1	309		146.1	189			127.7	0.3
2012	0	0	10.5	161.7								
2013	35.2	6.4	105.3	242.1	179.9	133.6	149.4	284.5		71.7		
2014	10.3	62.6	93.3	97.2	320.5	86.7	73.8	137.3	166	199.9	82.2	
2015	0	0.6	16.4	70.5	61.8	69.8	125.4	134.2	50.4	61.7	141.6	19.8
2016	2.3			105.7	21.9	0.5	2.5	11	1.4	1.6	1.9	
2017	0	0	77.5	67.3	281.5	53.2	176.5	148			8.7	0
2018	0				207.3	274				74.5	19	
2019	0	0	112.1	21.7	207	171.1	282.7			0	84	
2020	62	172.8			103.5	219.1	199.2	176.8				

Source: ENMA (2025)

7. Humbo Tebela Station

Year	Jan	Feb	Mar	Apr	May	Jun	Jul	Aug	Sep	Oct	Nov	Dec
1980								27.6				
1987												17.1
1988	52.3	50.9	36.8	219.4	84.7	125.2	250.1	213.3	23.7	111.6	0	12
1989	43.2	53.7	76	70.3	146.5	184.9	136.1		125.5	88.7	17.2	167.8
1990	8.4	153.8	85.2	69.2	115.5	46.7	91		90.9	34.3	15.9	26
1991	25.1	110.3	76.2	36.7	99	62.7	94	79.2		22.5	8.4	12
1992	4.5	27	93.5	155	67.8	58	194.7	188.7	82.3	100.5	42.7	18.7
1993		59.1	25.7	215.5	139.1	89.7	33	66.9	10.5	33	2.6	0
1994	0	25	64.3	103	178	215	257.2	121	55.5	125	78.5	8.4
1995	2	43.7	33.5	146.4	225.5	116.3	212.7	97.1	105.4	79.8	63.2	9.1
1996	34.6	7.6	155.3	196.3	195	333.1	202.5	377.5	261.6	39.3	50.8	0
1997	1.9	0	0	224.7	104.2	116.9	221.1	84.8	28.1	387	221.3	89.2
1998	156.4	44.3	82.1	88.6	108.6	211.5	133.3	205.1	63.1	162.8	13.3	4.1
1999	13.9	0	52.2	99.1		142.9	104.4	102.3	65.9	146.5	8.2	0
2000	5.8	0	21.8	147.1	324.1	117.7	184.3	144.4	95.4	123.4	62.1	11.4
2001	35.4	7	84.3	75.3	161.1	148.7	195	230.9	75.5	166.6	9.5	6.8
2002	68.2	7.1	82.3	131.7		41.8	86.7	198.5	62.3	9.7	39.1	253.1
2003	47.5	21.4	31	220.6	88.6	177.9	201.7	193	24	18.7	13.8	168.6
2004	118.7	11.3	17.6	158.3	24.3	65.2	148.9	84.9	21.1	53.5	22.5	4.7
2005	12.5	8.4	107.9	166.8	233.2	126.3	149.7	124.5	196	107.3	42.2	0
2006	3.6	41.2		215.7	101		87.1	204	64.3	150.3	46.9	42.2
2007	44.7	44.1	46.7	75.7	210.5	142.9	205	289.6	241.1	19	8.6	0
2008	14.5	19.2	0	85.6	139.7	93.3	189.6	169.2	209.8	198.9	169	6.7
2009	19.5	5.6	41.3	63.9	199.1	33.4	55.7	43.1	65.5	78.3		
2010	45.6	56.6	163.3	165.7	285.9	152.7	102.5	150.7	49.8	53	11.5	3.3
2011	0	9.6	86.8	17.7	247.6	93.3	156.3	177	211.6	78.7	147.8	0
2012	0	0	19.3	148.4	77.9	172	281.4	230.8	117.5	8.4	73.9	14.1
2013	15	0	84.7	158.1	241.1	103	233.9	111.9	87.8	122	56.3	0
2014	4.7	19.2	138	40.9	121.3	166.6	157.5	135		92.9	50.2	0
2015		0	115.2	99.7	158	99.1	99.2	49.5		75.1	115.5	76.4
2016	19.6	51.5	31.3	178.6	210.5	160.7	61.6	61	95.1	46	35.4	18.2
2017	0	2.6	38.1	42.4	163.9	43.5	228.5	189.8	128.7	222.9	21.9	0
2018	0	10.8	51		178.4	175.7	52.9	193.3		6.4	124.4	0
2019		0	10.2	47.3	119.9	316.7	192.4		139.5		203.1	
2020	20.8	60.9		99.4	150.8	111.7	101.8	66.9	33.6	9.7	3	
2021	0	44.7	3.7	55.1	69.1	9	31.2					
2022					44	24					6	0

Source: ENMA (2025)